scientific reports

OPEN

Silver nanoparticles synthesized using aerial part of *Achillea fragrantissima* and evaluation of their bioactivities

Mashail Fahad Alsayed[1], Hissah Abdulrahman Alodaini[1], Ibrahim M. Aziz[1✉], Rawan M. Alshalan[1], Humaira Rizwana[1], Fetoon Alkhelaiwi[1], Sara Mohammed ALSaigh[2] & Noorah A. Alkubaisi[1]

Achillea fragrantissima (*A. fragrantissima*), a desert plant, is used internally in Arabian traditional medicine to treat inflammatory, spasmodic gastrointestinal disorders, and hepatobiliary diseases. The study focuses on the environmentally friendly production of silver nanoparticles (AgNPs) from the water-based aerial parts of the *A. fragrantissima* plant and their ability to kill bacteria and cells. Ultraviolet-visible (UV-Vis) spectroscopy, scanning electron microscopy (SEM) with energy dispersive X-ray (EDX) analysis, transmission electron microscopy (TEM), and Fourier transform infrared spectroscopy (FTIR) were used to describe the AgNPs. They were then tested for their ability to fight cancer and bacteria. A change in colour from yellow to brown and a surface plasmon resonance peak at 440 nm, seen with UV-Vis spectroscopy, showed that AgNPs had formed. In a Gas Chromatography-Mass Spectrometry (GC-MS) test of the aerial parts of *A. fragrantissima*, twenty bioactive components were found. These included isolongifolol and 3E,10Z-Oxacyclotrideca-3,10-diene-2,7-dione, methylbuta-1,3-dienyl)-7-oxabicyclo [4.1.0] heptan-3-ol. The extract exhibited high phenolic and flavonoid content (77.52 ± 1.46 mg GAE/g dry weight and 59 ± 2.17 mg QE/g dry weight, respectively). According to the IC_{50} values of 17.2 ± 1.18 and 14 ± 2.43 µg/mL, the AgNPs had a lot of power to kill cancer cells from the MCF-7 and HepG2 lines. Some genes that cause cell death (*caspase-3*, *8*, *9*, and *Bax*) were turned on more in the treated cells compared to the control cells that had not been treated. These genes were *Bcl-xL* and *Bcl-2*. Additionally, substantial activity against both Gram-positive bacteria and Gram-negative bacteria was found by antibacterial screening. Overall, this study underscores *A. fragrantissima's* diverse biological activity and its potential in drug discovery and nanomedicine, promoting the development of natural antibacterial and anticancer therapies.

Keywords Medicinal plants, AgNPs, Antibacterial activity, Cytotoxicity, Apoptosis

Plants produce a variety of secondary metabolites that, with the help of modern analytical tools, allow for the scientific examination of these plants, uncovering compounds beneficial for treating various illnesses[1]. These metabolites display numerous biological effects, such as antibacterial, antioxidant, and anticancer properties, making them highly beneficial for human health and well-being[2].

The diverse flora of Saudi Arabia represents a valuable genetic resource for agricultural and medicinal plants in the Arabian Peninsula[3]. Due to its unique phytogeographical features, Saudi Arabia possesses a rich array of medicinal and aromatic plants, with approximately 30% being rare[4]. Traditional medicine remains prevalent in many regions of Saudi Arabia, employing different plant components to treat common diseases[5].

The *Achillea* L. genus, which is a member of the *Asteraceae* family, comprises approximately 100 species of wild plants that are utilized as medicinal plants worldwide. These plants have been used for thousands of years to cure a broad range of illnesses[6]. The *Achillea* plant is extensively found in Saudi Arabia's northern areas, namely in the provinces of Tabuk and Arar[7].

In plants of *A. fragrantissima*, phenolic acids (protocatechuic, vanilic, chlorogenic, ferulic and quinic acid), flavonoids (apigenin, apigeninglucoside, apigenin-rutinoside and apigenin-neohesperioside, luteolin, vitexin

[1]Department of Botany and Microbiology, College of Science, King Saud University, 11451 Riyadh, Saudi Arabia. [2]Department of Clinical Laboratory Sciences, College of Applied Medical Sciences, King Saud University, P.O. Box 10219, 11433 Riyadh, Saudi Arabia. ✉email: iaziz@ksu.edu.sa

and vitexin-rhamnoside, cirsiliol, diosmetin, chrysoplenetin, chrysophanol D), lignans (sesamin), terpenic lactones (achillolid A) and alkamides (pellitorin, 8,9-Z-dehydropellitorin, anacyclin) have been found as mainly bioactive compounds [17–20]. Many essential oils of *Achillea* were used to describe several bioactive metabolites, including phenolic acids, flavonoids, lignans, terpenes, and alkamide. Several biological properties are shown by *Achillea* species, including angiogenic[8], antifungal[9], antibacterial[10], antioxidant[11], and antimicrobial[12] activity.

A. fragrantissima is one of the most often used and important medicinal herbs in Arabic traditional medicine, used to make medicinal teas meant to prevent and treat a broad range of health concerns[11]. The following conditions have been treated with these plants: diabetes, dysmenorrhea (painful menstruation), smallpox, eye infections, fever, headache, and exhaustion. Among the plants used in traditional therapeutic methods is *A. fragrantissima*, which is well known for its medicinal qualities. Furthermore, *A. fragrantissima* is a physiologically active plant that has antibacterial, anti-inflammatory, and antioxidant properties[13–16]. *A. fragrantissima* essential oil has antibacterial capabilities that may affect Gram-negative *Escherichia coli* and Gram-positive bacteria such as *Staphylococcus aureus*, *S. epidermidis*, and *Bacillus subtilis*. Gram-negative bacteria were often less sensitive to *A. fragrantissima's* essential oil than Gram-positive bacteria[13,17,18]. The main bioactive substances found in *A. fragrantissima* plants are phenolic acids (protocatechuic, vanilic, chlorogenic, ferulic, and quinic acid), flavonoids (luteolin, vitexin, and vitexin-rhamnoside, cirsiliol, diosmetin, chrysoplenetin, chrysophanol D), lignans (sesamin), terpenic lactones (achillolid A), and alkamides (pellitorin, 8,9-Z-dehydropellitorin, anacyclin)[11,19].

Concerning the *Achillea* genus, uncommon species are used to synthesize NPs, including *A. biederteinii*[20], *A. wilhelmssi* CKoch (Aw)[21], and *A. millefolium*[22]. Interestingly, the cytotoxic and bactericidal qualities of *A. millefolium* extracts have only partially been understood by a small number of experimental studies in the field of *A. millefolium* research. The aerial parts of the *A. fragrantissima* extract that were collected from the Tabuk and Arar regions exhibited antibacterial and antioxidant properties[7]. Our study fills a substantial gap in the field despite the abundance of material available on *A. fragrantissima* extracts since not much scientific research has been conducted regarding this plant despite its well-known traditional medicinal benefits. Gas Chromatography-Mass Spectrometry (GC-MS) is a cutting-edge method for comprehensive chemical analysis that reveals a distinct and complex chemical makeup. This study quantifies the amounts of total phenolic content (TPC) and total flavonoid content (TFC) and offers compelling evidence of the extract's potent anticancer and antibacterial effects. These findings provide new light on the potential therapeutic applications *of A. fragrantissima*, especially in connection to the extract's potent antibacterial activity against various strains and capacity to cause apoptosis in cancer cell lines. Moreover, the current research is focused on the environmentally friendly synthesis of AgNPs from *A. fragrantissima*. In this work, we aimed to identify the most prominent bioactive components in the aerial part of the *A. fragrantissima* plant using GC–MS analysis. Additionally, it seeks to assess the potential effects of synthetic AgNPs against MCF-7 breast cancer cells and hepatocellular carcinoma (HepG2) cells in comparison to the aqueous extract of *A. fragrantissima*. Furthermore, it seeks to elucidate the underlying mechanism by utilizing the reverse transcription polymerase chain reaction (RT-PCR) based mRNA expression profile of specific pro- and anti-apoptosis marker genes. Additionally, the minimum inhibitory concentration (MIC) and minimum bactericidal concentration (MBC) techniques were used to assess the antibacterial efficacy of the synthesized AgNPs and *A. fragrantissima* aqueous extract against both Gram-positive and Gram-negative bacteria.

Results
The biogenic attributes of AgNPs synthesized from aqueous *A. fragrantissima* aerial part extract

The synthesized AgNPs were evaluated using UV–Vis spectroscopy, and the results showed a strong peak at 442 nm, which is suggestive of the AgNPs-associated surface plasmon resonance (SPR) band. In comparison to AgNPs, the UV spectra of the crude extract had the lowest absorption (300 nm), which indicated the formation of AgNPs from *A. fragrantissima* aerial part extract (Fig. 1). As shown in Fig. 1, the synthesized AgNPs occurred through the reduction of Ag + to Ag^0, resulting in a noticeable change in the color of the mixture from light yellow to dark brown.

Data from a Nicolet 6700 Fourier transform infrared spectroscopy (FTIR) scanning was collected between 4000 and 400 cm^{-1}. As shown in (Fig. 2; Table 1), the synthesis AgNP spectra revealed absorbance peaks at 3440, 2098, 1650, 794, and 442.7 cm^{-1}. FTIR studies revealed four functional groups in *A. fragrantissima* aerial component extract: three functional groups at 3442, 750, and 490 cm^{-1} were identical to those reported in the synthesis of AgNPs for alcohol, 1,2-disubstituted, and Halo compounds, and another unique functional group was detected at 1734 cm^{-1} for cyclopentanone compounds.

The produced AgNPs were inspected using a JEM-1011 scanning electron microscopy (SEM) and a variety of spectroscopic tests including UV-Vis spectroscopy and an energy-dispersive X-ray (EDX). The qualitative and quantitative state of each ingredient involved in the synthetic process was evaluated using EDX analysis and SEM imaging. The morphological features of the synthesized AgNPs were visible in the SEM images shown in (Fig. 3A). The EDX spectra indicated main peaks of 2.983 Kev in the silver region, accounting for 9.23% of the mass (Fig. 3B). SPR peak in the absorption spectra shows a red shift due to the agglomeration of AgNPs. Notably, there were extremely faint signals at 0.227 and 0.525 Kev, respectively, for the two peaks corresponding to the carbon and oxygen atoms.

The TEM imaging and particle size distribution analysis were used to confirm the UV-Vis results to quantify the particle size range and surface shape of the synthesized AgNPs obtained from *A. fragrantissima* aerial parts. The findings showed that AgNPs are prone to aggregation and were mostly spherical. The sizes on average varied between 16 and 22 nm (Fig. 4).
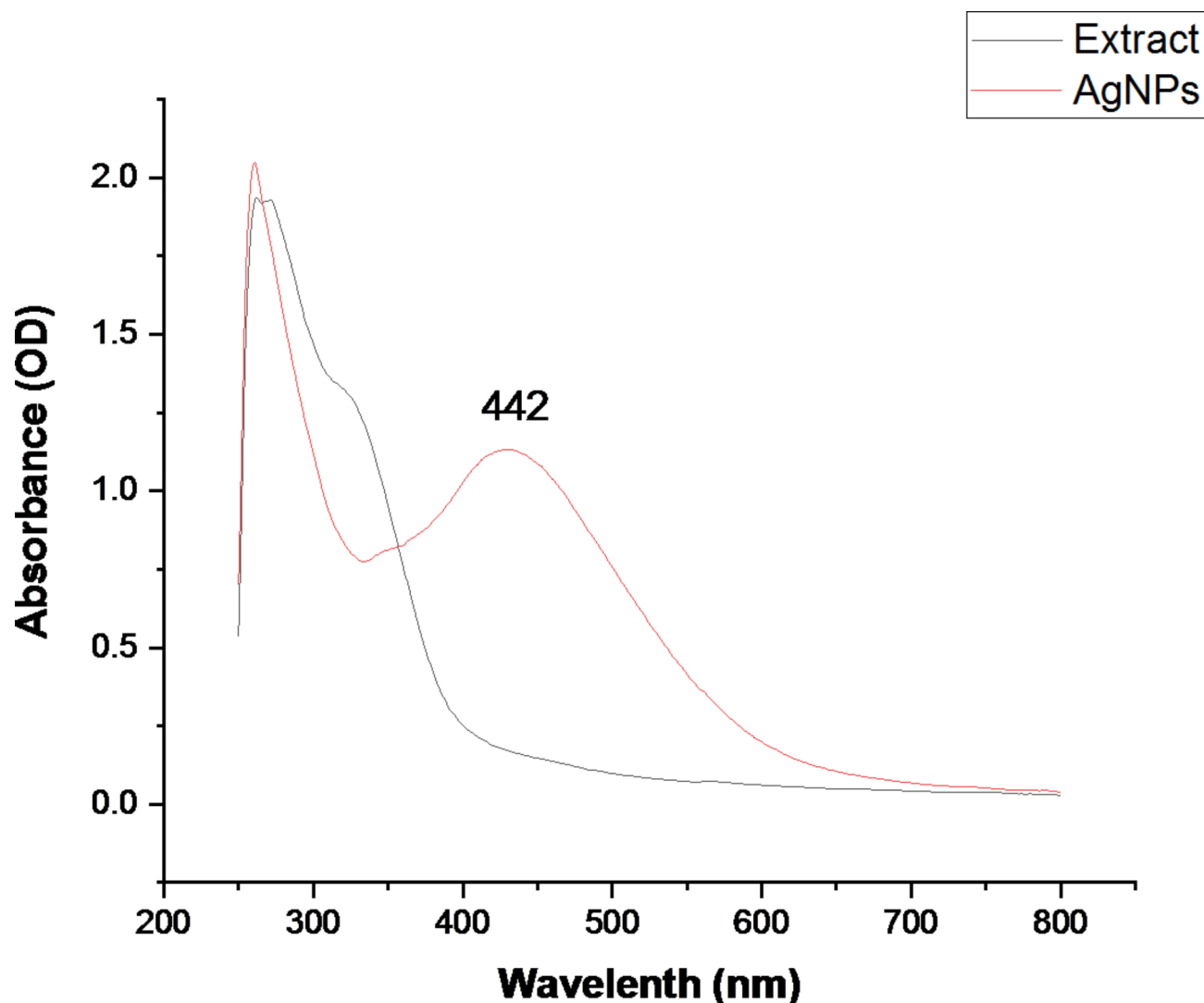
Fig. 1. UV-Vis spectroscopy of the synthesized *A. fragrantissima* AgNPs compared to the crude extract.

GC-MS analysis of aqueous *A. fragrantissima* aerial part extract

In a GC-MS analysis, the composition of bioactive components extracted from the aqueous extract of *A. fragrantissima* was determined. The molecular formula (MF), concentration (peak area percentage), retention time (RT), and concentration of the active principles are shown in (Table 2; Fig. 5). Twenty different bioactive substances were identified. The main bioactive component in the aqueous extract was found to be (3E,10Z)-Oxacyclotrideca-3,10-diene-2,7-dione (16.97%), followed by (methylbuta-1,3-dienyl)-7-oxabicyclo [4.1.0] heptan-3-ol (4.77%) and isolongifolol (4.48%).

TPC and TFC in aqueous extract analysis

A. fragrantissima's aqueous extract's TPC and TFC were determined calorimetrically. Using the Folin–Ciocalteu technique, the aqueous extract had the greatest TPC (77.52 ± 1.46 mg GAE/g dry weight of the dry extract; $R^2 = 0.989$) (Fig. 6A), whereas the aluminum chloride (AlCl$_3$) assay yielded TFC of 59 ± 2.17 mg QE/g dry weight of the dry extract ($R^2 = 0.992$) (Fig. 6B).

Cell cytotoxicity

The cytotoxic potential of the *A. fragrantissima* extract and synthesized AgNPs on human cancer cells was investigated using the MCF-7 (Fig. 7A) and HepG2 (Fig. 7B) cell lines. The MTT test was used to measure the cytotoxic effects after exposing the cells to different concentrations (0–400 µg/mL) of the synthesized AgNPs and the extract from the aerial part of *A. fragrantissima* for 24 h. The results of the MTT experiment showed that both the synthesized AgNPs and the aerial part of the *A. fragrantissima* extract decreased cell viability in a dose- and time-dependent manner. It's important to note that the cytotoxic activity reduced when 100 µg/mL of synthesized AgNPs were added to the culture medium. Cell viability is reduced with increasing extract concentration. The synthesized AgNPs significantly reduced the viability of MCF-7 cells to about $25.27 \pm 2.49\%$
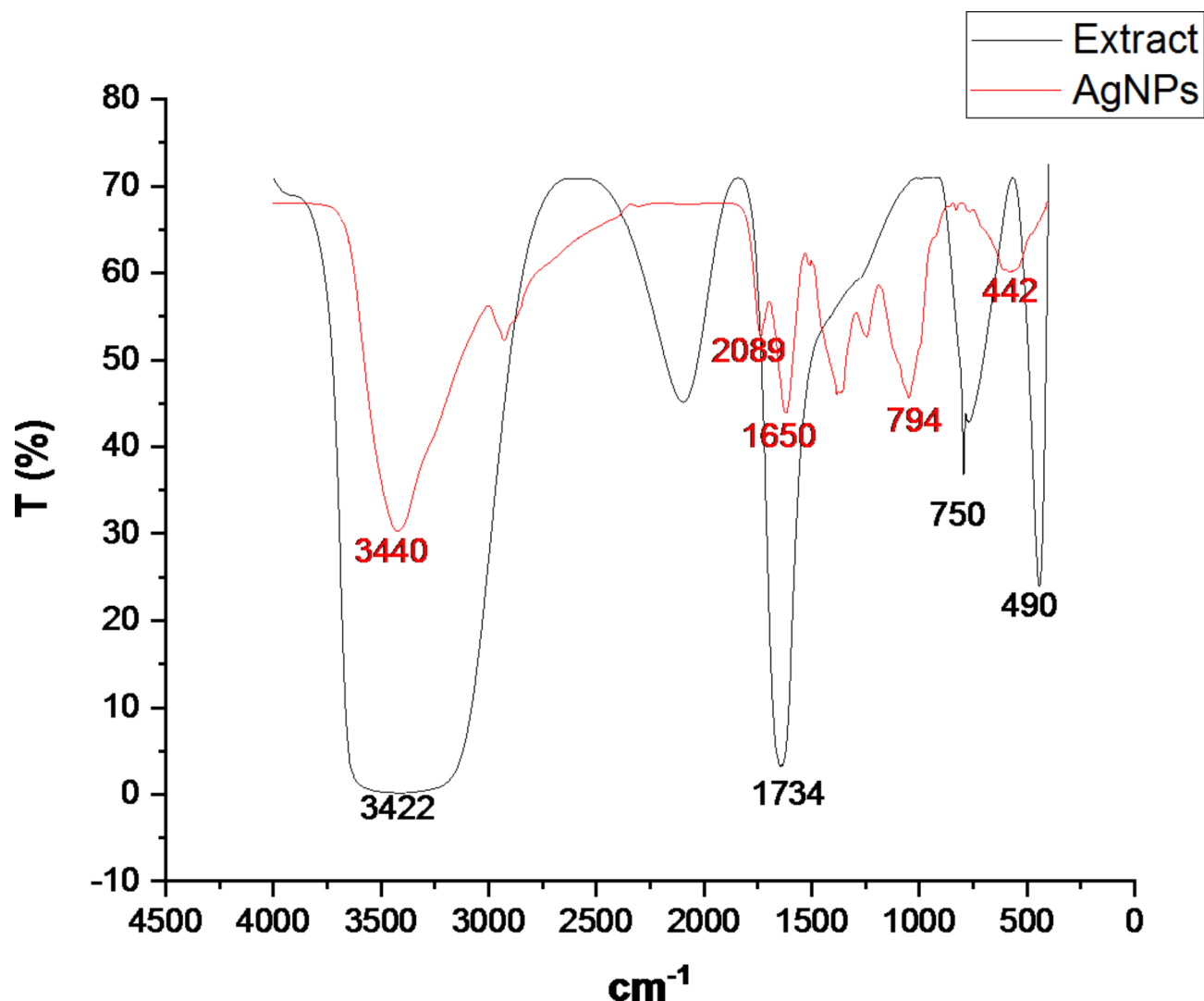
Fig. 2. FTIR spectra synthesis AgNPs from the extract of aerial parts of *A. fragrantissima*.

Treatment	Spectra	Functional group	Compound class	Shape and strength
AgNPs	3440	O-H stretching	Alcohol	Strong, broad
	2089	N=C=S stretching	Isothiocyanate	strong, broad
	1650	N-H bending	Amine	Medium, broad
	794	C-H bending	halo compound	Strong, sharp
	442	C-Cl stretching	Halo compound	Medium, sharp
A. fragrantissima aerial part extract	3442	O-H stretching	Alcohol	Strong, broad
	1734	C=O stretching	Cyclopentanone	Strong, broad
	750	C-H bending	1,2-disubstituted	Strong, sharp
	490	C-Cl stretching	Halo compound	Medium, sharp

Table 1. Functional groups produced by FTIR analysis.

and $18.07 \pm 1.19\%$ at 400 μg/mL, with IC_{50} values of 17.2 ± 1.18 μg/mL for MCF-7 and 14 ± 2.43 μg/mL for HepG2, compared to the untreated cells ($P < 0.05$). However, the IC_{50} values for the aqueous aerial part of the *A. fragrantissima* extract were 36.2 ± 2.19 μg/mL for HepG2 and 24.5 ± 1.16 μg/mL for MCF-7.

Apoptotic analysis

The level of apoptosis induced by *A. fragrantissima's* aqueous extract and AgNP-treated MCF-7 and HepG2 cells was compared to untreated control cells. This comparison further confirmed the presence of apoptosis. The
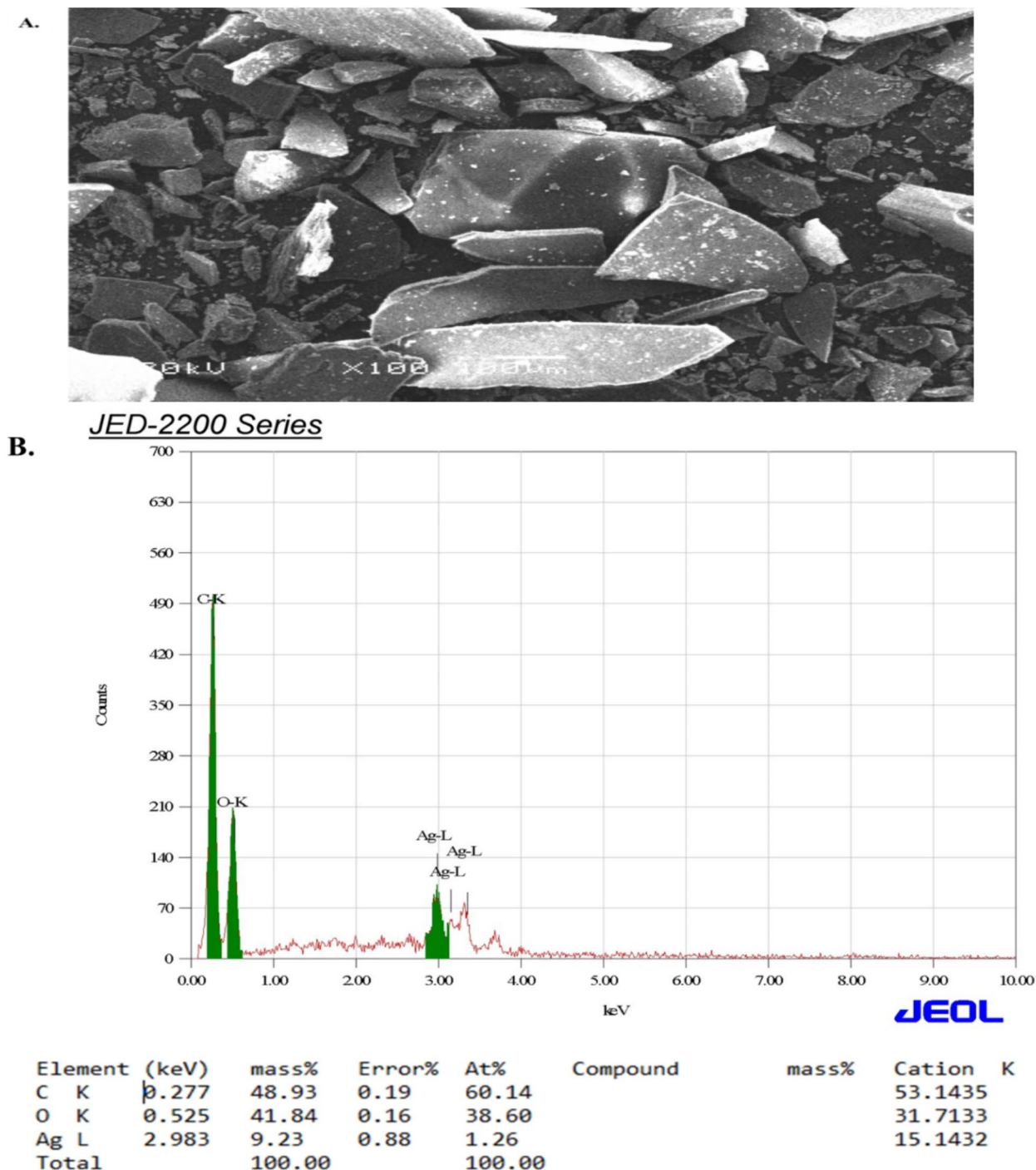
Element	(keV)	mass%	Error%	At%	Compound	mass%	Cation	K
C K	0.277	48.93	0.19	60.14			53.1435	
O K	0.525	41.84	0.16	38.60			31.7133	
Ag L	2.983	9.23	0.88	1.26			15.1432	
Total		100.00		100.00				

Fig. 3. SEM image (**A**) and EDX (**B**) analysis of the synthesized AgNPs obtained from *A. fragrantissima* aerial parts.

expression of anti-apoptotic genes (*Bcl-xL* and *Bcl-2*) was lower than that of the untreated control ($P < 0.05$), while the activities of caspase 3, 8, and 9 were four times higher in cells exposed to synthesized AgNPs compared to the control (untreated cells) (Refer to Fig. 8A and B).

Cells morphemically change

The aqueous extract of *A. fragrantissima* and the MCF-7 and HepG2 cell lines to observe the morphemic changes of the synthetic AgNPs. Following treatment with an aqueous extract of A. fragrantissima and synthetic AgNPs, MCF-7 and HepG2 cells were cultured in a humid environment incubator (37 °C, 5% CO_2, 95% air). After 48 h of treatment, Mock, MCF-7, and HepG2 cells treated with an aqueous extract of *A. fragrantissima* and synthetic
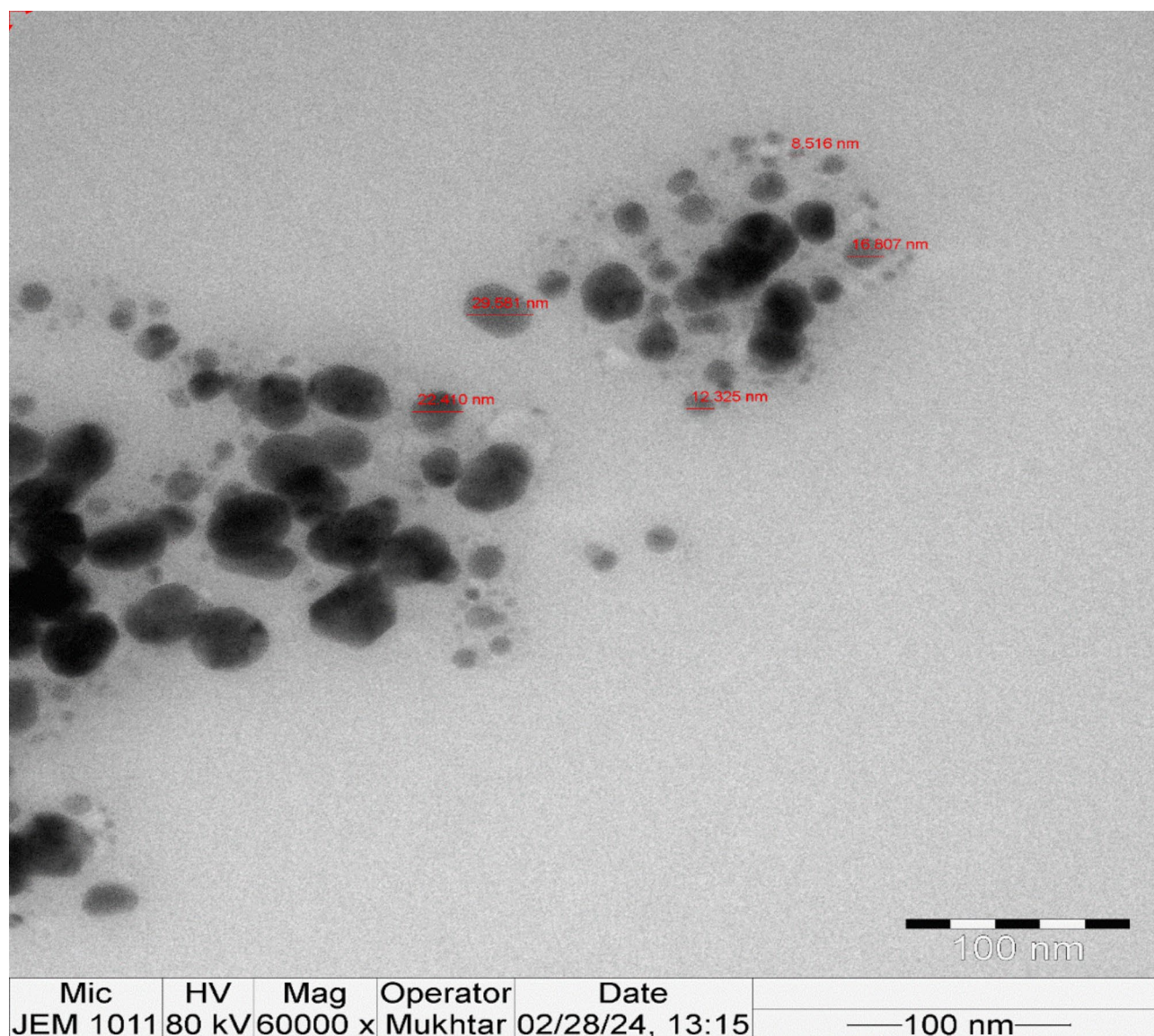
Fig. 4. TEM of the synthesized AgNPs obtained from *A. fragrantissima* aerial part.

AgNPs showed morphological alterations including rounding of the cells, the development of tiny aggregates, and the progressive detachment of the AgNPs (Fig. 9C and F). On the other hand, little morphological alterations appeared in MCF-7 and HepG2 cells that were exposed to aerial parts of *A. fragrantissima* extract (Fig. 9B and E) as compared to untreated cells (Fig. 9A and D).

Antibacterial effects of bioactive compounds

The study examined the antibacterial activity of *A. fragrantissima* extract's aerial parts and synthesized AgNPs against both Gram-positive and Gram-negative bacteria, including *S. aureus*, *S. epidermidis*, and *E. faecalis*, as well *as E. coli*, *K. pneumoniae*, and *P. aeruginosa*. The findings demonstrated that, when tested against the tested bacteria, disc diffusion synthesized AgNPs exhibited more antibacterial activity (Table 3; Fig. 10) than the aqueous extract of *A. fragrantissima* (Table 4; Fig. 11). The minimum inhibitory concentration (MIC) values for the Aqueous Extract of *A. fragrantissima* ranged from 12.5 ± 0.00 to 50 ± 0.00 μg/mL, while the range of MIC values for synthesized AgNPs was 2.34 ± 0.00 to 9.37 ± 4.41 μg/mL. When tested against *P. aeruginosa* (MTCC 27853), the lowest MIC value for the synthetic AgNPs was 2.34 ± 0.00 μg/mL. When tested against *S. aureus* (MTCC 29213), the highest MIC value for the synthetic AgNPs was 9.37 ± 4.41 μg/mL. Therefore, the present results suggest that the synthesized AgNPs are more highly sensitive against Gram-negative bacteria particularly *P. aeruginosa* than Gram-positive bacteria.

Discussion

Nanotechnologies have revolutionized various fields of science, including medical and pharmaceutical technology, physics, engineering, and chemistry. NPs typically measuring between one and one hundred nanometers, can

Peak	Rt	Area	Area %	Start time	End time	Name	MF
1	15.44	931,610	3.69	15.09	15.69	Propanenitrile, 3-(5-diethylamino-1-methyl-3-pentynyloxy)-	$C_{13}H_{22}N_2O$
2	16.154	753,422	2.99	15.71	16.334	1 H-imidazole-2-methanol, 1-decyl-	$C_{14}H_{26}N_2O$
3	16.527	6,728,503	26.7	16.38	16.85	Z, Z-2,5-Pentadecadien-1-ol	$C_{15}H_{28}O$
4	17.33	741,079	2.94	17.13	17.46	11,13-Dimethyl-12-tetradecen-1-ol acetate	$C_{18}H_{34}O_2$
5	18.04	986,455	3.91	17.87	18.32	Acetamide, N-(6-acetylaminobenzothiazol-2-yl)-2-(adamantan-1-yl)-	$C_{21}H_{25}N_3O_2S$
6	18.609	4,277,176	16.97	18.32	19.22	(3E,10Z)-Oxacyclotrideca-3,10-diene-2,7-dione	$C_{12}H_{16}O_3$
7	24.461	665,399	2.64	24.39	24.59	(2R,3R,4aR,5 S,8aS)-2-Hydroxy-4a,5-dimethyl-3-(prop-1-en-2-yl)octahydronaphthalen-1(2 H)-one	C15H24O2
8	24.834	1,130,670	4.48	24.74	24.94	Isolongifolol	$C_{15}H_{26}O$
9	24.987	801,544	3.18	24.94	25.22	Acetamide, N-methyl-N-[4-(3-hydroxypyrrolidinyl)-2-butynyl]-	$C_{11}H_{18}N_2O_2$
10	26.903	1,052,508	4.17	26.84	26.96	Acetic acid, 6-hydroxymethyl-cyclodecyl ester	$C_{13}H_{24}O_3$
11	26.998	538,377	2.13	26.96	27.11	2-Myristynoyl-glycinamide	$C_{16}H_{28}N_2O_2$
12	27.719	488,807	1.93	27.58	27.85	2 H-3,9a-Methano-1-benzoxepin, octahydro-2,2,5a,9-tetramethyl-, [3R-(3α,5aα,9α,9aα)]-	$C_{15}H_{26}O$
13	28.409	841,450	3.33	28.32	28.62	Aminoacetamide, N-methyl-N-[4-(1-pyrrolidinyl)-2-butynyl]-	$C_{11}H_{19}N_3O$
14	28.83	837,998	3.32	28.71	29.03	i-Propyl 9-tetradecenoate	$C_{17}H_{32}O_2$
15	29.298	659,265	2.61	29.19	29.42	4-Hydroxy-β-ionone	$C_{13}H_{20}O_2$
16	30.558	752,230	2.98	30.49	30.70	4-(3-Hydroxy-2,6,6-trimethylcyclohex-1-enyl)pent-3-en-2-one	$C_{14}H_{22}O_2$
17	30.865	836,095	3.31	30.70	31.01	2,6-Di-t-butyloctahydroazulene-3a,8-diol	$C_{18}H_{34}O_2$
18	33.81	339,570	1.34	33.71	33.91	2-Methyl-E, E-3,13-octadecadien-1-ol	$C_{19}H_{36}O$
19	34.238	1,203,719	4.77	34.09	34.44	: 2,2,6-Trimethyl-1-(3-methylbuta-1,3-dienyl)-7-oxabicyclo[4.1.0]heptan-3-ol	$C_{14}H_{22}O_2$
20	35.9	631,736	2.51	35.81	36.18	1,3-Benzenedicarboxylic acid, 5-(1,1-dimethylethyl)-	$C_{12}H_{14}O_4$

Table 2. GC-MS analysis of bioactive compounds identified from the extract *A. fragrantissima* aerial parts.

interact with a wide range of biomolecules, including proteins and nucleic acids, due to their small size. This allows NPs to either evade immune system detection or flow past cells. Metal NPs have been used extensively in biology and medicine in recent years[23]. Green synthesis techniques are environmentally friendly methods for synthesizing nanomaterials. Recently, a variety of biological substrates have been used to create metal and metal oxide-based nanomaterials, including plant extracts, fungi, and bacteria[24]. Based on the widespread interest in metallic NPs, this study aimed to characterize and investigate the cytotoxic and antibacterial effects of AgNPs synthesized using *A. fragrantissima* aerial parts extract.

The size and shape of NPs in aqueous solutions are often examined using UV-Vis spectroscopy[25]. AgNPs-containing solutions are also known to exhibit a distinctive absorption peak in the 420–480 nm region[26]. The synthesized of AgNPs using an aqueous extract from the aerial part of the *A. fragrantissima* extract exhibited an effective reduction of silver ions to NPs, evidenced by a color shift and confirmed through spectroscopic and microscopic methods The activation of the SPR, action, and the decrease of $AgNO_3$ may be the cause of the emergence of the dark brown color[27].

There were two peaks in the UV-Vis spectra of the *A. fragrantissima* extract and synthesized AgNPs, appearing at 300 and 442 nm (Fig. 1). The first peak showed at 300 nm due to the autochrome and chromophore substituent n → π* transitions localized inside the ring of the cinnamoyl and benzoyl system. Generally, this transition, which related to double bounds, was specific to flavone nuclei of extract compounds[28–30]. The second peak showed at 442 nm by a prominent absorption peak in the UV-Vis absorption spectra, which is suggestive of the AgNPs-associated SPR band (Fig. 1). This absorption is close to the absorbance peaks reported by[31] and[32] to synthesize AgNPs using green methods.

Important details regarding the chemical composition and biophysical characteristics of this natural extract, as well as its possible uses in nanotechnology and medicine, are revealed by the combined analysis of FTIR spectroscopy and biogenic synthesis of AgNPs using *A. fragrantissima* aerial part extract.

Five main functional groups were identified from synthesis AgNPs by FTIR analysis: hydroxyl (O-H) stretching at 3440 cm⁻¹, N=C=S stretching at 2089 cm⁻¹, N-H bending at 1650 cm⁻¹, C-H bending at 794 cm⁻¹ and C-Cl stretching at 442 cm⁻¹. These functional groups indicate the existence of alcohols, alkene compounds, amines, and halogen compounds, respectively. For *A. fragrantissima* aerial part extract, FTIR studies identified four functional groups. Three functional groups at 3442, 750, and 490 cm⁻¹ were identical to those in synthetic AgNPs for alcohol, 1,2-disubstituted, and halo compounds. Another distinct functional group was found at 1734 cm⁻¹ for cyclopentanone molecules.

The strong and wide absorption band at 3441 cm⁻¹, indicates the presence of numerous hydroxyl groups, possibly related to phenolic chemicals in the aerial part extract. By identifying these functional groups, the chemical composition of the aerial component extract of *A. fragrantissima* is revealed, providing valuable information that may direct future investigations into the plant's biological activity and potential therapeutic applications.

In the study conducted by Eid et al. (2020). the FTIR analysis of root samples of *A. fragrantissima* extract revealed strong absorption for the functional groups of N–H aliphatic primary amine, carboxylic acid (OH) stretch, C-H asymmetric stretching vibration for aliphatic groups, and C–N stretching vibrations for aromatic and aliphatic amines[33].
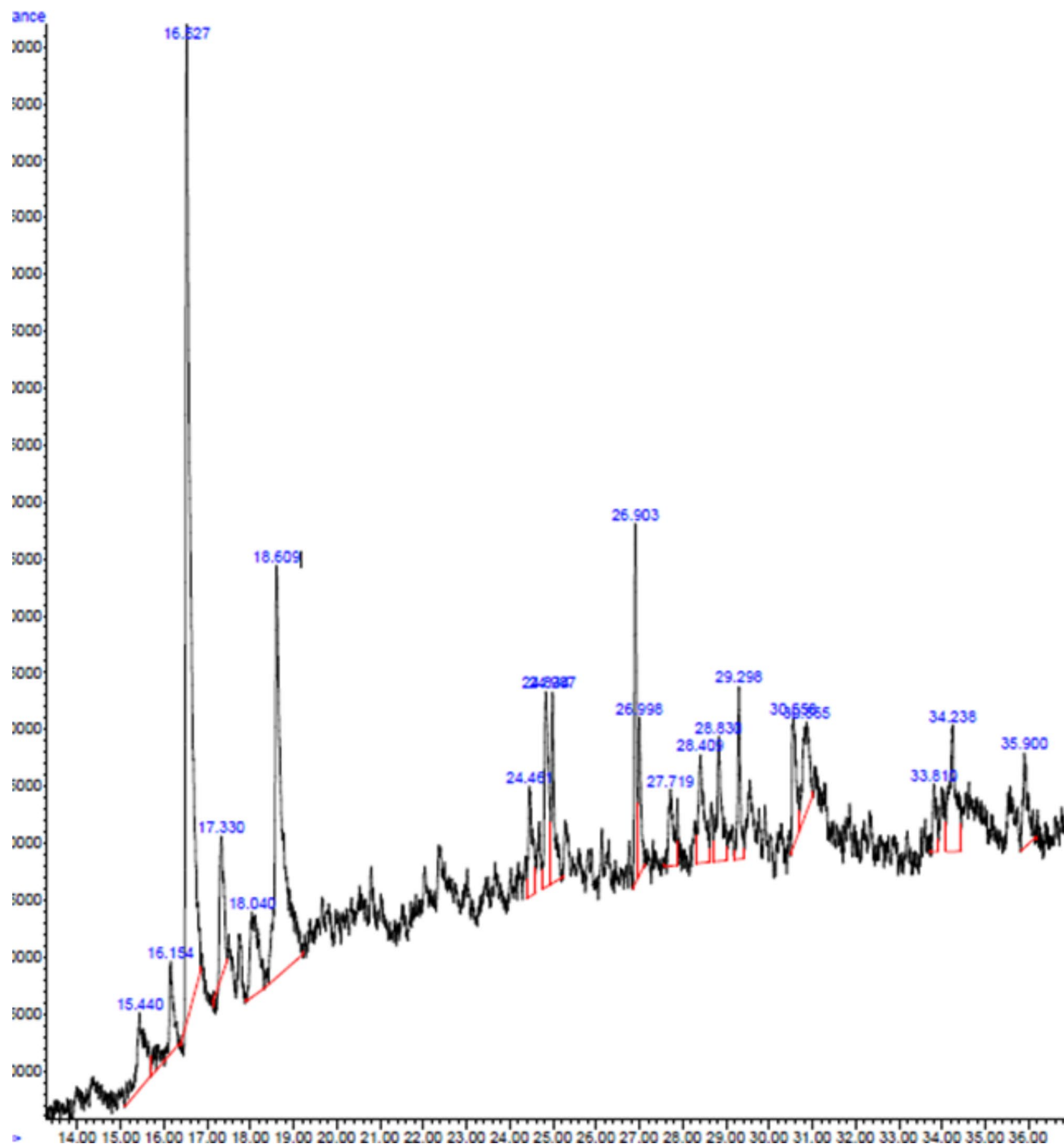
Fig. 5. GC-MS spectrum of the aqueous extract of *A. fragrantissima*. The GC-MS apparatus was set for 73 min, and an aqueous extract was used for the study. Every detected peak in the spectrum designates a recognized chemical, and the existence of a sizable peak denotes the extract's major component.

SEM imaging revealed the morphological features of the AgNPs, and EDX analysis confirmed that silver was the major element present, with a distinctive peak at 2.983 keV, compatible with the absorption peak observed in the UV-visible spectrophotometer. The low contamination from the biomolecules in the aerial component extract employed for the synthesis is further shown by the weak signals corresponding to carbon and oxygen atoms, underscoring the purity of the generated AgNPs. This study's TEM images demonstrated the production of spherical AgNPs with an average particle size of 16 to 22 nm. It has been reported that the AgNPs using aqueous extracts of *A. maritima* and *A. millefolium* had average diameters of around 21 nm and 22.4 nm, respectively[22,34]. These findings demonstrate that the type of plant extract and the experimental setup have an impact on the size of silver NPs[31].
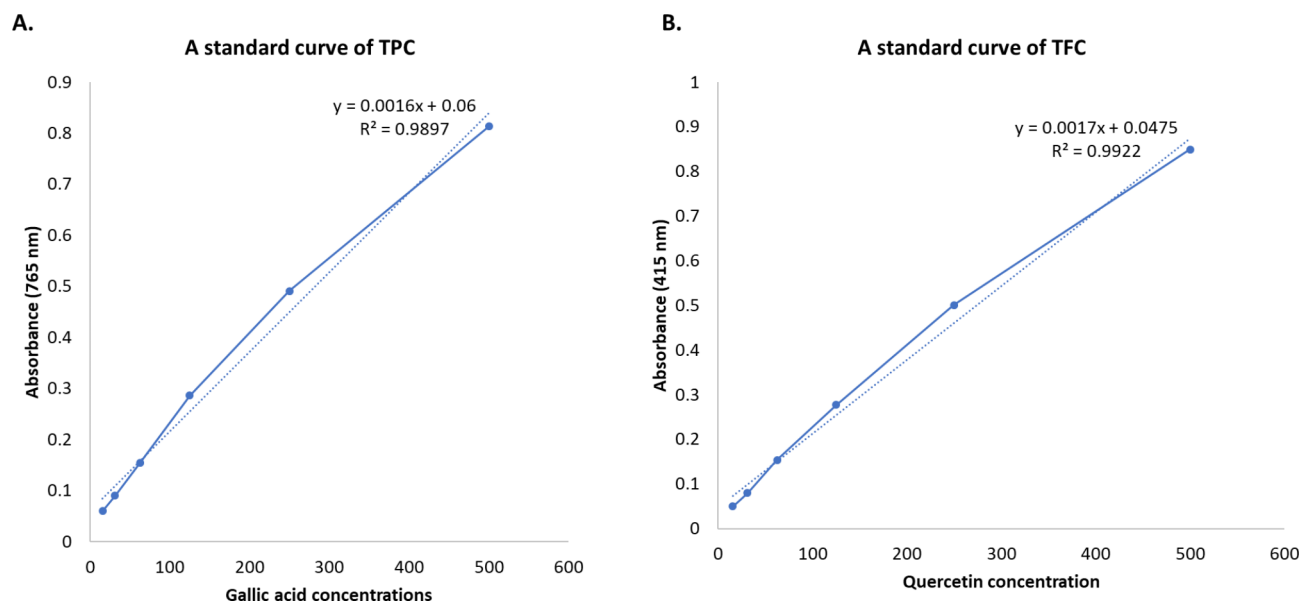
A.

B.

Fig. 6. A standard curve of TPC (**A**), and TFC (**B**) were determined calorimetrically.
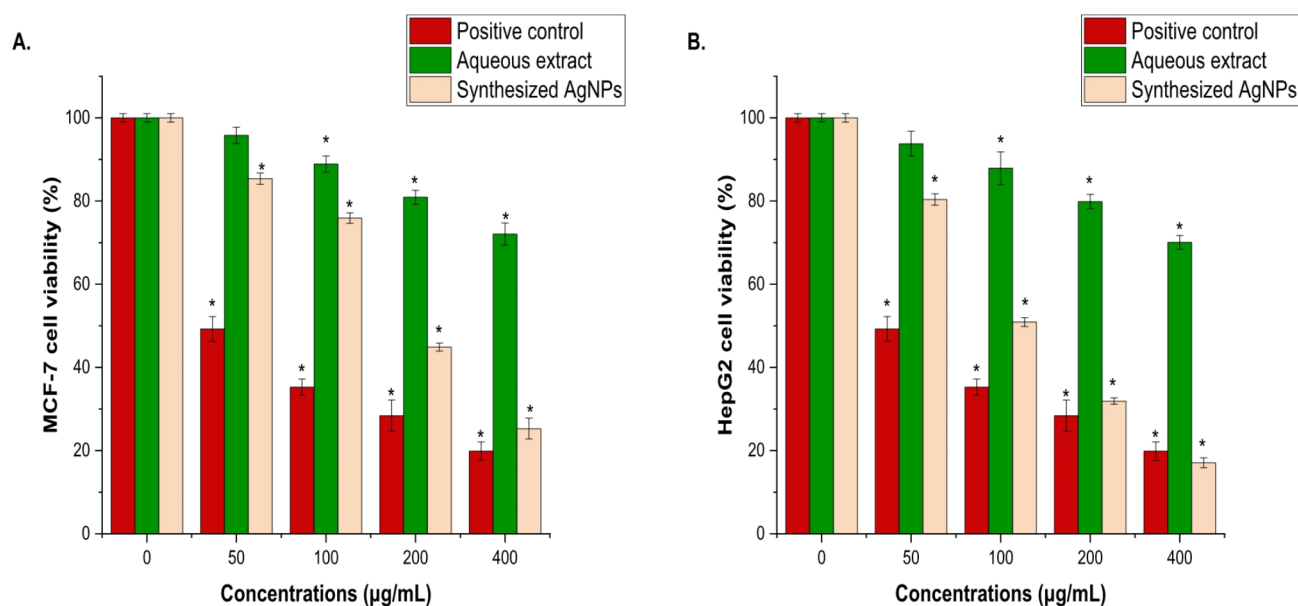
A.

B.

Fig. 7. The effect of the aqueous extract of *A. fragrantissima* and synthesized AgNPs on the viability of MCF-7 (**A**), and HepG2 cells, (**B**), was examined using the MTT assay. Cells were treated with aqueous extract of *A. fragrantissima* and synthesized AgNPs (0–400 µg/mL) for 24 h. Mean ± SD is presented from three independent experiments, (* = $P < 0.05$ compared to non-treated cells (control)).

The GC-MS analysis of *A. fragrantissima* aerial part extract revealed a diverse array of bioactive components, encompassing twenty compounds including 3E,10Z-Oxacyclotrideca-3,10-diene-2,7-dione, methylbuta-1,3-dienyl)-7-oxabicyclo [4.1.0] heptan-3-ol, and isolongifolol which are shown in Fig. 5; Table 2. The biological effects of several of these compounds have been previously researched, indicating interesting areas for further study. This could be due to the compound's chemical structure containing ester and phenol groups[35]. Hirasawa et al. (2016) concluded that certain macrolide antibiotics have significant lethal effects on head and neck squamous carcinoma cell lines when exposed to nutrient-deprived conditions[36]. These compounds' presence in
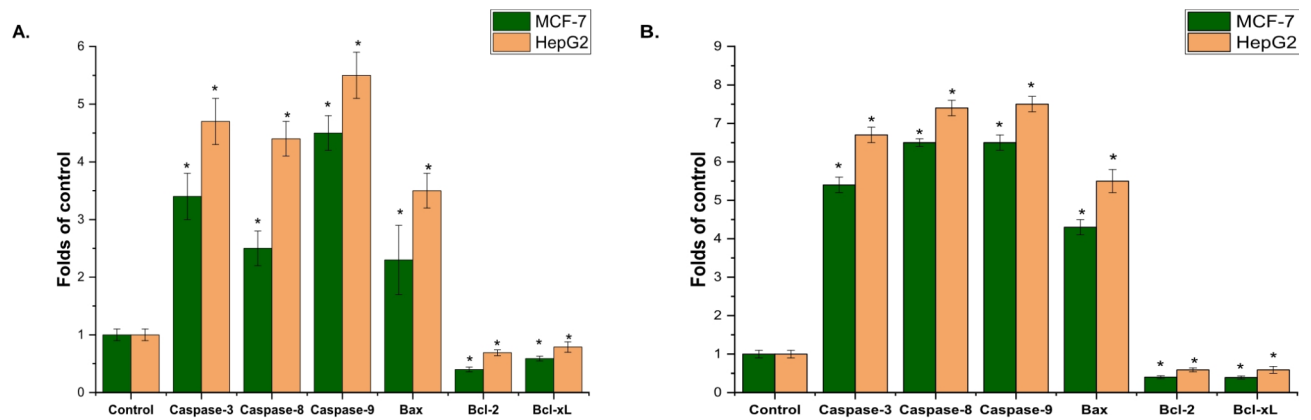
Fig. 8. Effect of aqueous extract of *A. fragrantissima* (50 μg/mL), (**A**), and synthesized AgNPs (15 μg/mL). (**B**) on MCF-7 and HepG2 cell lines. Synthesized AgNPs treated MCF-7 and HepG2 cells showed an increased percentage of the apoptotic population (*caspase-3*, *8*, *9*, and *Bax*) after 24 h incubation. The results are represented as the mean ± SD of three independent experiments, (* = $P < 0.05$ compared to non-treated cells (control)).
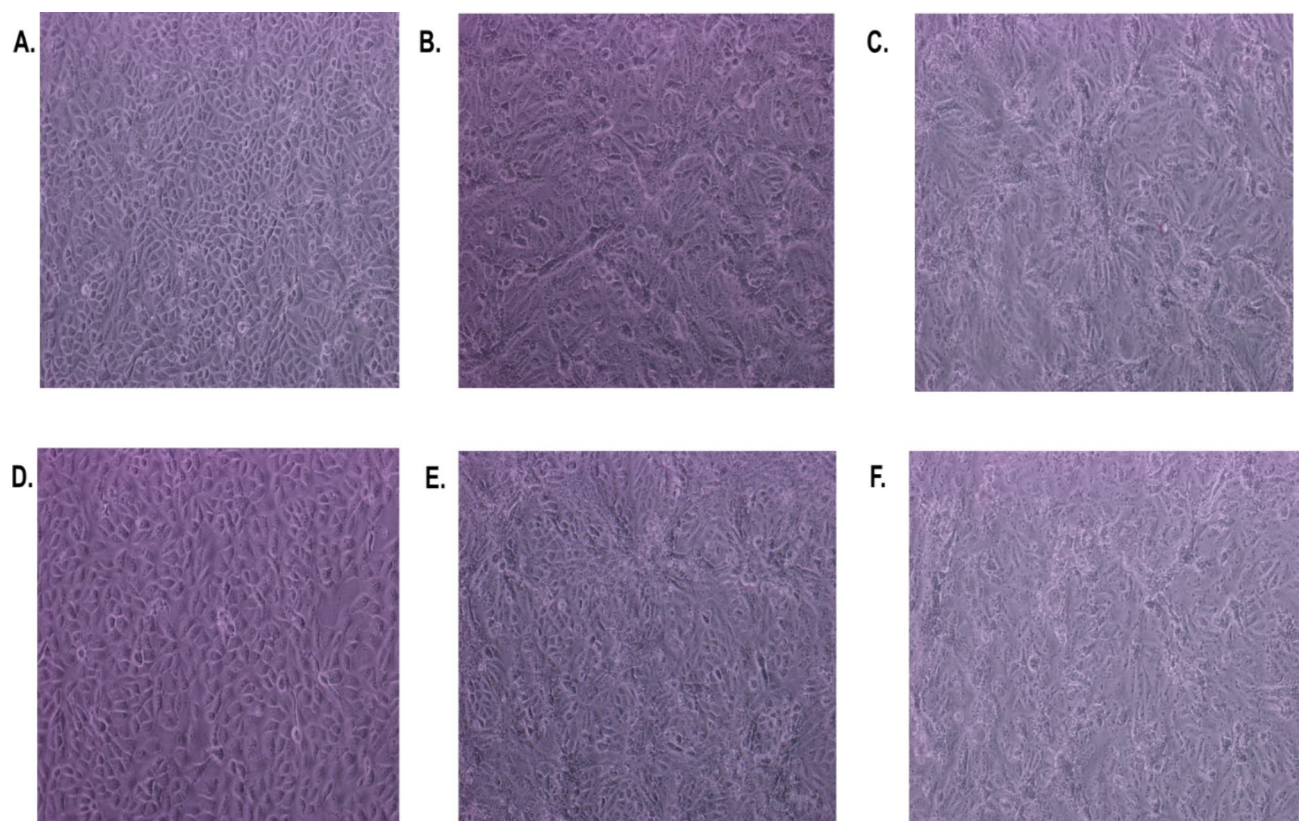

Fig. 9. The effect of aqueous extract of *A. fragrantissima* and synthesized AgNPs on the MCF-7 and HepG2 cells morphology, cells treated with 50 μg/mL, and 15 μg/mL, respectively for 48 h (**A**) represents MCF-7 non-treated cells, (**B**) = represents MCF-7-treated cells with aqueous extract, (**C**) represents MCF-7 -treated cells with synthesized AgNPs, (**D**) = represents HepG2 non-treated cells, (**E**) represents HepG2 treated cells with aqueous extract, (**F**) = represents HepG2 treated cells with synthesized AgNPs.

Bacterium/Dilution	Positive control	400 μg/mL	200 μg/mL	100 μg/mL	50 μg/mL	MIC (μg/mL)	MBC (μg/mL)
S. aureus (MTCC 29213)	HS	S	MS	MS	LS	25 ± 0.00	50 ± 0.00
S. epidermidis (MTCC 12228)	HS	S	MS	MS	MS	12.5 ± 0.00	25 ± 0.00
E. faecalis (ATCC-29212)	HS	MS	LS	LS	LS	25 ± 0.00	50 ± 0.00
E. coli (ATCC 25922)	HS	S	MS	MS	LS	25 ± 0.00	50 ± 0.00
K. pneumoniae (MTCC 13883)	HS	MS	LS	LS	LS	50 ± 0.00	100 ± 0.00
P. aeruginosa (MTCC 27853)	HS	S	MS	MS	LS	25 ± 0.00	50 ± 0.00

Table 3. The inhibitory zone, MIC, and minimum bactericidal concentration (MBC) of the aerial part of the *A. fragrantissima* extract. LS = low sensitivity, MS = moderate sensitivity, S = sensitivity, HS = high sensitivity.
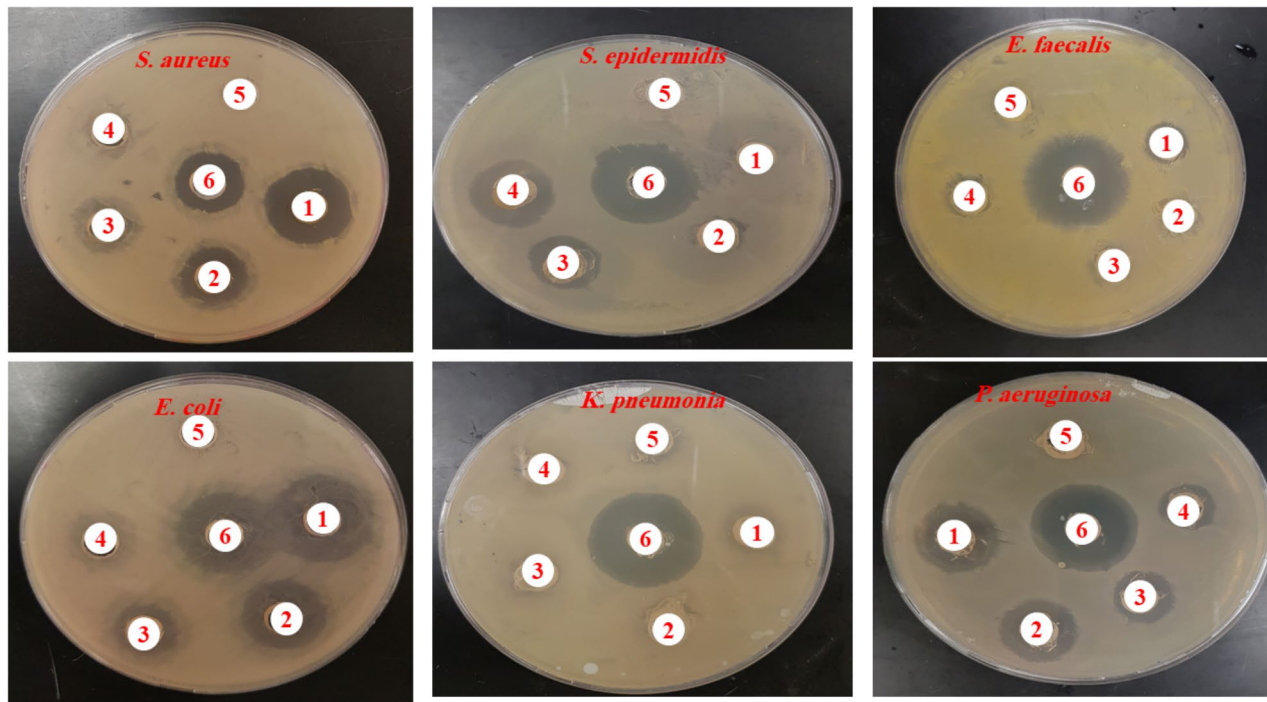

Fig. 10. Antibiogram demonstrating the antibacterial activity of aqueous extract of *A. fragrantissima* against selected bacteria strains. (**1**) denotes 400 μg/ml; (**2**) denotes 200 μg/ml; (**3**) denotes 100 μg/ml; (**4**) denotes 50 μg/ml; (**5**) denotes the negative control; (**6**) denotes the ciprofloxacin (positive control).

Bacterium/Dilution	Positive control	400 μg/mL	200 μg/mL	100 μg/mL	50 μg/mL	MIC (μg/mL)	MBC (μg/mL)
S. aureus (MTCC 29213)	HS	HS	S	S	MS	9.37 ± 4.41	12.25 ± 0.00
S. epidermidis (MTCC 12228)	HS	HS	S	S	MS	4.68 ± 2.21	6.25 ± 0.00
E. faecalis (ATCC-29212)	HS	S	MS	MS	LS	4.68 ± 2.21	6.25 ± 0.00
E. coli (ATCC 25922)	HS	HS	S	S	S	4.68 ± 2.21	6.25 ± 0.00
K. pneumoniae (MTCC 13883)	HS	HS	S	S	S	3.12 ± 0.00	6.25 ± 0.00
P. aeruginosa (MTCC 27853)	HS	HS	HS	S	S	2.34 ± 0.00	3.12 ± 0.00

Table 4. The inhibitory zone, MIC, and MBC of the synthesized AgNPs. LS = low sensitivity, MS = moderate sensitivity, S = sensitivity, HS = high sensitivity.

A. fragrantissima aerial part extract indicates that the plant has potential as a natural antibacterial and anticancer agent. Understanding the modes of action and possible therapeutic applications of these medications, both alone and in combination, requires further study. Awad et al. isolated piceol, eupatilin 7-methyl ether, chrysosplenol D, cirsiliol, and cirsimaritin from A. fragrantissima leaves methanolic extract and tested on MCF-7, HepG2, A549, HeLa (cervix adenocarcinoma), and PC3 (prostatic adenocarcinoma) cell lines, with IC_{50} values ranging from 3.2 to 28.3 μg/mL[37]. Additionally, a recent study revealed that the main components of the aerial parts of *A.*
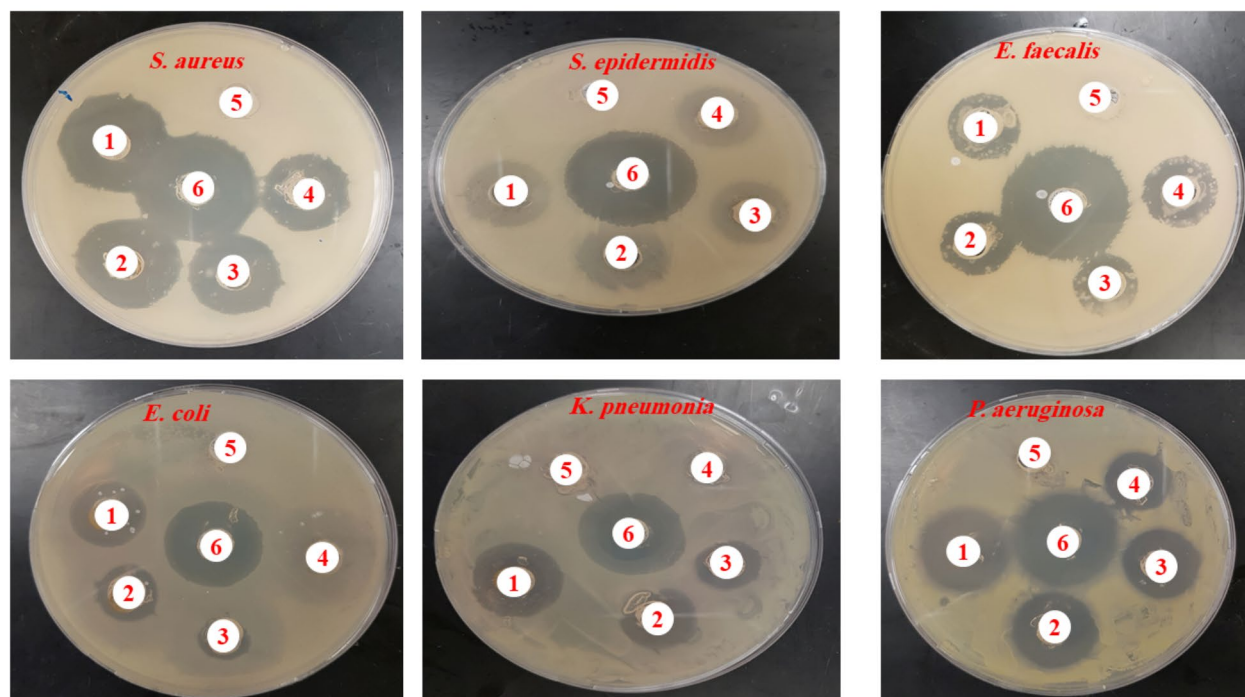
Fig. 11. Antibiogram demonstrating the antibacterial activity of synthesized AgNPs against selected bacteria strains. (**1**) denotes 400 µg/ml; (**2**) denotes 200 µg/ml; (**3**) denotes 100 µg/ml; (**4**) denotes 50 µg/ml; (**5**) denotes the negative control; (**6**) denotes the ciprofloxacin (positive control).

fragrantissima essential oils were α-thujone, myrcenyl acetate, artemisia ketone, β-thujone, lavandulol, santolina alcohol, and 3-thujanone. These were collected from Wadi Hagool, Suez, Egypt, and Wadi Harqan, Alqareenah, Riyadh Region, Saudi Arabia[38].

Flavonoids are phenolic compounds isolated from a wide range of plants. They have various pharmacological roles, including cardiovascular protection, anti-inflammatory, anticancer, antioxidant, antimicrobial, feeding repellent, and light screening properties[39]. In our investigation, we discovered that the TFC of the dry extract was measured to be 59 ± 2.17 mg of quercetin equivalents per gram of dry weight of the extract, and the TPC was determined to be 77.52 ± 1.46 mg per gram of dry weight of the extract. These phenolic compounds are essential for protecting cells and tissues from damage caused by oxidative stress and for scavenging free radicals[40].

The cytotoxicity of the aqueous aerial parts of the *A. fragrantissima* extract and synthesized AgNPs was evaluated on human cancer cell lines MCF-7 and HepG2. The MTT test findings showed a dose- and time-dependent reduction in cell viability compared to untreated cells. The IC_{50} values were 17.2 ± 1.18 µg/mL and 36.2 ± 2.19 µg/mL in MCF-7 and 14 ± 2.43 µg/mL and 24.5 ± 1.16 µg/mL in HepG2 caused by synthesized AgNPs and the crude extract. The apoptosis analysis confirmed these findings. Caspase 3, 8, and 9 activity was significantly higher in cells treated with A. fragrantissima aerial parts or synthesized AgNPs compared to the control group. Additionally, treated cells showed lower expression of anti-apoptotic genes Bcl-xL and Bcl-2 than untreated controls. This indicates that both treatments induce apoptosis in cancer cells, leading to their harmful effects. Only a few researches have revealed the anticancer effects of *A. fragrantissima* crude extracts in cancer cell lines. Previous research tested *A. fragrantissima* leaves methanolic extract against K562 (myeloid leukemia), Jurkat (T-cell leukemia), and HepG2 (hepatocarinoma) cells and showed dramatic morphological alterations and loss of viability in K562 cells[41]. Break et al. (2021) treated HepG2, A549 (lung carcinoma), HCT-116 (colorectal carcinoma), and MCF-7 (hormone-dependent breast cancer) cells with methanolic extract of *A. fragrantissima* leaves and reported cytotoxic bioactivity of the extract against A549 cells with induction of apoptosis, including *caspase-3* activation, increased p53 and Bax expression, and down-regulation of Bcl-2 expression[42]. A recent study indicated that the dichloromethane extract of *A. fragrantissima* flower was proven to be the strongest agent leading to MDA-MB-231 cell proliferation with IC_{50} values of 32.43 ± 3.41 µg/mL, followed by leaf-derived extracts with values of 36.67 ± 3.94 µg/mL[43]. Previous investigation has shown the strong anticancer potential of AgNPs utilizing *A. biebersteinii* flower extract with an IC_{50} value of 20 µg/mL by inhibiting particular cell cycle genes and simulating programmed cell death genes of MCF-7 cell line[20]. Recently, the synthesized AgNPs exhibited higher cytotoxicity (793.3% and 77.2% at 250 µg/mL) against MCF-7 and Hep-G2 cancer cells, respectively, in comparison to the leaf extract of *Lallemantia royleana*[44]. AgNPs synthesized from *Rotheca serrata* (L.) Steane & Mabb. Flower bud extract exhibited strong anticancer effectiveness against the pancreatic ductal adenocarinoma cell line with an IC_{50} value of 36.01 µg/mL[45].

Our research offers an approach for treating cancer that depends on the production of genes that trigger apoptosis. This research used MCF-7 and HepG2 cancer cells as models to demonstrate the apoptotic capabilities

of *A. fragrantissima*. In fact, after treating *A. fragrantissima*, we looked for the expressions of apoptotic regulators. Moving further, the first screening confirms and signals that rising *A. fragrantissima* concentrations cause cell cytotoxicity and activated apoptotic network genes (*Caspase-3*, *Caspase-8*, *Caspase-9*, and *Bax*) in MCF-7 and HepG2 cells. Consequently, the viability nature of the cell decreases[37,46]. Our findings match with the results reported by Alasmari, A. (2024)[16]. Our research and these studies' results indicated that *A. fragrantissima* could treat cancer cells in cancer cells by dose-dependent cytotoxicity and apoptosis analysis.

In the present study, the antibacterial efficacy of aerial parts of the *A. fragrantissima* extract and synthesized AgNPs against bacterial strains was studied against Gram-positive bacteria (*S. aureus*, *S. epidermidis*, and *E. faecalis*) and Gram-negative bacteria (*E. coli*, *K. pneumoniae*, and *P. aeruginosa*). The MIC values for aerial parts of the *(A) fragrantissima* extract varied from 12.5 ± 0.00 to 50 ± 0.00 µg/mL. The MIC values for synthesized AgNPs ranged from 2.34 ± 0.00 to 9.37 ± 4.41 µg/ml. *P. aeruginosa* was more susceptible to synthetic AgNPs (MIC value = 2.34 ± 0.00 µg/mL). Likewise, *P. aeruginosa* was more susceptible to the C-AgNPs obtained from the extract of *Cardamine hirsuta* L. leaf[47]. Whereas, *(B) subtilis* showed greater susceptibility to the synthesis of AgNPs using the leaf extract of *Ixora brachypoda* DC. among the microbial pathogens tested[48]. Based on our data, it is generally known that most AgNPs have more antibacterial activity against Gram-negative bacteria than Gram-positive bacteria. These results match a previous work in which the synthesis of AgNPs from the root extract of *Astragalus tribuloides* was demonstrated to have better inhibitory effects against strains of Gram-positive bacteria (*B. cereus* and *S. aureus*) than against strains of Gram-negative bacteria (*E. coli* and *Shigella flexneri*)[49]. A similar trend was observed by the AgNPs synthesized from *Otostegia persica* (Burm.) Boiss. Leaf extract exhibited significant antimicrobial efficacy against the Gram-negative bacteria (*E. coli*, *P. aeruginosa*, and *Salmonella typhi*) as compared with the Gram-positive bacteria strains (*S. aureus*, *B. subtilis*, and *Streptococcus pyogenes*)[50]. In contrast, a previous study showed that AgCl-NPs synthesized from a *Pulicaria vulgaris* Gaertn. The aerial part extract had more inhibitory activity against the Gram-positive *S. aureus* strain compared to the Gram-negative *E. coli* strain[51]. These findings may be explained by Gram-positive bacteria's thick peptidoglycan layer, which restricts AgNP penetration into cells. These results might be explained by the cellular wall's strong peptidoglycan layer of Gram-positive bacteria, which limits the possibilities of AgNP penetration into cells[40]. On the other hand, previous research indicated that the change of Gram-negative bacteria lipopolysaccharides (LPS) with AgNPs, due to the negative charge of LPS, promotes NPs adhesion[52]. Many researchers emphasize the basic mechanism of action of NPs, which includes electrostatic interaction between the negative charge of the microbial cell membrane and the positive or smaller charge of AgNPs[52,53]. Elsharkawy et al. (2021) found that flowering aerial parts of *(A) fragmentissimaa* had good antibacterial activity against Gram-positive bacteria, including (*S. epidermidis*, *(B) cereus*, and *S. aureus* clinical isolate), antibacterial activity ranging between high to no activity (between 14.5 ± 0.5–6.0 ± 0.0 mm zone of inhibition)[7]. Furthermore, *A. fragrantissima* essential oil inhibited bacterial growth in both Gram-positive and Gram-negative bacteria, particularly *E. coli* and *S. epidermidis*[38]. AgNPs synthesized from *A. maritima* exhibited antibacterial activity against *E. coli* and *S. typhi*, with 15.8 and 14.5 mm zone inhibition diameters, respectively[52]. Overall, our findings support the use of the aerial part of the *A. fragrantissima* and synthetic AgNPs as effective antibacterial agents.

We acknowledge the shortcomings and limitations in terms of the methodology we used in our present study. Polar and non-polar volatile compounds need the study of dual-capillary polar and polar columns. To confirm the newly identified compounds, retention indices of the constituents must be computed by linear interpolation in connection to the retention times of two standard mixes of n-alkanes (C_8–C_{20} and C_{21}–C_{40}). One limitation of the study is the absence of in-vivo investigations. In vivo research is crucial for complementing in vitro data, especially when evaluating the potential biological effects of plant extracts against pathogenic bacteria/fungi and their anti-proliferative activity against cell lines. The in vivo environment is significantly more complex in terms of target organ delivery, effectiveness, and potential side effects. Future research should prioritize in-vivo investigations to establish the efficacy and safety of these compounds.

In conclusion, *A. fragrantissima* aerial part extract contains several bioactive chemicals with significant antioxidant, anticancer, and antibacterial properties. Unlike previous reports, this study is unique in demonstrating that the synthesized AgNPs showed potential anticancer effects at lower doses, indicating increased caspase activity and decreased anti-apoptotic gene expression in treated cells, confirming apoptosis and antimicrobial activities against Gram-positive and Gram-negative species, particularly *P. aeruginosa*. These findings provide a solid foundation for future study into its therapeutic applications and possibilities for the development of natural pharmaceutical products. Future research should concentrate on in-vivo studies to assess the effectiveness and safety of these substances.

Methods
Preparation of aqueous plant extract

The aerial parts of *A. fragrantissima*, which include the stems, leaves, petioles, flowers, fruit, and seeds, were purchased at the Riyadh market in Saudi Arabia in September of 2023. *A. fragrantissima* is a little plant that grows forever. White, woolly plants have upright, up to one-meter-tall stems that are heavily branched from the base; the many, herbaceous, terete, and stiff blooming branches form part of the plant. The leaves exhibit characteristics of being white to greyish-green in colour, tiny, thick, sessile, ovate, oblong, or oblong-lanceolate, with a rounded apex and gently undulating edges that are shallowly dentate and short mucronate. The plant is hairy and has a pleasant scent; the flower heads are terminal discoid and made up of many tubular florets; the ray florets are yellow and extremely short. Flowering period: from June to September. The plant was identified by Professor Dr. Mohammed Fasil of King Saud University's Department of Botany and Microbiology in Riyadh, Saudi Arabia. The voucher specimen was deposited at the Herbarium of the Department of Botany and Microbiology (KSU NO-18811).

The aerial parts of the *A. fragrantissima* were thoroughly cleaned using distilled water after being washed several times with tap water to remove dust. After air drying at room temperature for a week, the plants were ground into a fine powder using a grinder. Twenty grams of powdered aerial parts were suspended in 100 ml of distilled water in a beaker and left to stand at room temperature for 24 h. The extract was filtered in a conical flask using Whatman Grade 1 Filter Paper and refrigerated at 4 °C. This solution was used to synthesize AgNPs.

Green Synthesis of AgNPs from the Extract

Following the method outlined by[52], with slight modifications, the synthesis of AgNPs was carried out by adding 2 ml of the *A. fragrantissima* aerial parts to 100 ml of $AgNO_3$ (2 mM). The mixture was heated to 70 °C and stirred with a magnetic stirrer on a hotplate until the solution's color changed from light yellow to dark brown, as shown in (Fig. 12). The synthesized AgNPs were then recovered by centrifugation at 5,000 rpm and 4 °C for 30 min. After several rounds of centrifugation under the same conditions, the resulting pellet was purified using sterile Milli-Q water. The dried AgNPs were kept at 4 °C until use.

Characterization of AgNPs

Different techniques have been used to characterize the synthesized AgNPs. Initially, AgNPs were confirmed with a UV–Vis spectroscopy (Shimadzu UV-1800, Kyoto, Japan) in the 300–800 nm range with a plot interval of 1.0 nm, following the manufacturer's instructions and previous research findings[54]. The experiment was conducted in triplicate.

The elemental analysis and chemical composition of the AgNPs were determined using an SEM integrated with EDX analysis. Briefly, 5 µL of the pure AgNPs solution at a concentration of 0.1 mg/ml was coated onto carbon tape. The samples were allowed to air dry at room temperature for fifteen minutes. SEM imaging was carried out using a JSM-6380 LA SEM (JEOL LTD., Tokyo, Japan) following the manufacturer's instructions, and previous research (Singh and Mijakovic, 2022). The Smile ShotTM software provided optimal operating settings and seamless changeover between SEM and EDX. The JSM-6380 has a configurable GUI interface that makes the instrument easy to use.
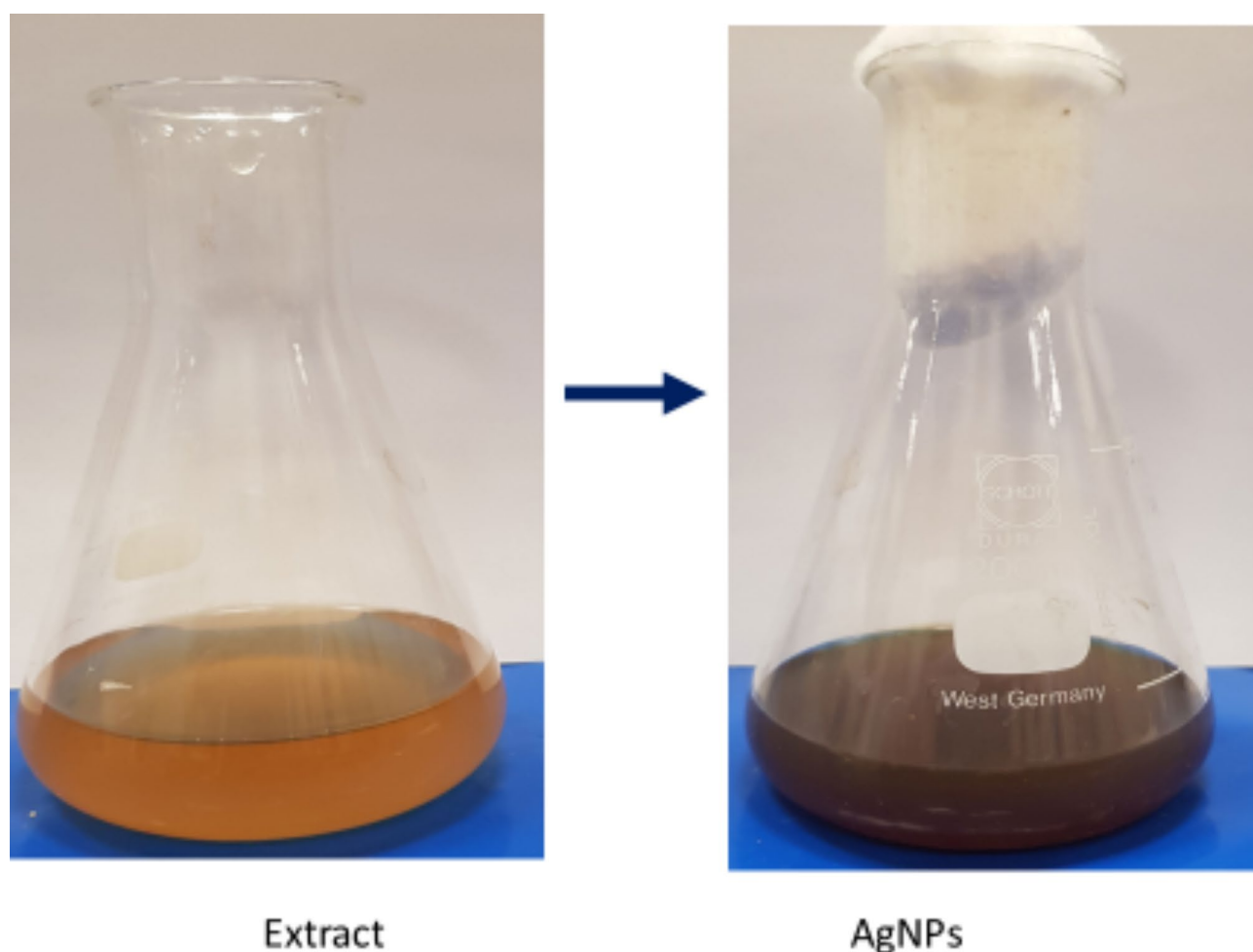

Extract → AgNPs

Fig. 12. Color change during the synthesis of the *A. fragrantissima* AgNPs.

The crystalline structure of the AgNPs was examined using a TEM (JEOL Ltd. Inc., Tokyo, Japan). Slide preparation and processing were conducted according to the manufacturer's instructions, as documented in previous research[55].

To confirm the potential impact of the various bioactive found in *A. fragrantissima*, an FTIR (Thermo Fisher Scientific, MS, USA) equipped with Omnic software was used to analyze the surface modification of the synthesized AgNPs. Following the manufacturer's instructions, measurements were taken over a range of 500–4000 cm^{-1}. The obtained wavelengths were analyzed using the FTIR Functional Group Database InstaNANO to identify potential functional groups based on peak height and shape (https://instanano.com/all/characterization/ftir/ftir-functional-group-search/, accessed May 12, 2024).

Determination of bioactive components of extract

Using the autosampler injection system, 0.9 µL of the *A. fragrantissima* aqueous extract diluted with acetone at a 1: 9 volume ratio, was injected for analysis using the (GC–MS) technique from Agilent Technologies Inc. (Santa Clara, CA, USA). The compounds were identified using a connecting database program. The disintegration of the material into its parts using gas chromatography and a mass selective detector GC-MS. A DB-5 MS capillary column from Agilent Technologies (30 m in length, 0.25 mm internal diameter, and 0.25 µm phase thickness) was used to separate the target chemicals.

The oven temperature ranged from 50 to 250 °C and a total analysis duration of 73 min. Helium was used as the carrier gas at a flow rate of 1 mL/min with an inlet temperature of 250 °C. The MS detector was configured with an acquisition scan type, scanning masses between 40 and 500 g/mol, a scan speed of 1.56, a solvent delay of two minutes, and an MS source temperature of 230 °C. The basis for the component identification method was provided by Willey and the National Institute of Standards and Technology (NIST) Libraries. Comparing the components with those found in the computer libraries (Willey and NIST) connected to the GC-MS instrument allowed for the identification of those with a matching factor of more than 90%.

TPC and TFC in aqueous extracts

The TPC in the aqueous extract was determined using a modifiedFolin–Ciocalteu method as described by[56]. The extracts were diluted to the appropriate concentration, and 0.25 mL volumes of theFolin–Ciocalteu reagent (diluted ten times with distilled water) and 7.5% $NaHCO_3$ were mixed. The mixture was incubated for 15 min at 45 °C, and the absorbance was measured at 765 nm using (U2001 UV–Vis Spectrophotometer, Hitachi, Japan). A standard curve was created using gallic acid concentrations between 20 and 200 µg/mL. The results were expressed in gallic acid equivalents (mg GAE/g per gram of extract).

The TFC in the aqueous extract was measured using the $AlCl_3$ colorimetric method, based on the formation of a flavonoid-aluminum complex with maximum absorption at 415 nm as described by[57]. In brief, 0.5 mL of the aqueous extract was mixed with 1.5 mL of methanol. The samples were then mixed with 0.1 mL of 10% $AlCl_3$ and 0.1 mL of 1.0 M sodium acetate. After incubating at room temperature in the dark for one hour, the absorption was measured at λmax 415 nm using a U2001 UV–Vis Spectrophotometer (Hitachi, Japan). Vitamin C was used as the positive control. The same process was used to create a calibration curve for the quercetin solution. The results were expressed as the mean ($\pm$ SD) amount of QE per gram of extract, based on three independent readings.

Cytotoxicity and apoptosis assay

The human hepatoma HepG2 (ATCC HB-8065) cell lines were selected for this study as functional in vitro model systems to test the cytotoxic effects of different plant extracts[58,59]. The cells were cultured in Dulbecco's Modified Eagle's Medium supplemented with 10% fetal bovine serum, 2 mM glutamine, and a 1% antibiotic solution with 100 U/mL of penicillin and 100 µg/mL of streptomycin. The cells were then kept at 37 °C in an atmosphere with 5% CO_2 and 95% air.

MCF-7 cells and HepG2 were seeded onto a 96-well plate and incubated overnight at 95% humidity, and 5% CO_2 at 37 °C. After 24 h, to ensure cell adhesion and confluence in the wells, the medium was replaced with a fresh medium containing different concentrations of AgNPs (1–100 µg/mL) with cisplatin (30 µg/mL) as the positive control for 48 h. The effects of aqueous extract and AgNPs on MCF-7 and HepG2 cell viability were assessed using (MTT) assay (Life Technologies, Eugene, Oregon, USA). Briefly, cells were seeded in a 96-well plate (Corning Costar, Lowell, NY, USA) at a density of 1×10^4 cells per well and treated with different concentrations of the aqueous extract (0–500 µg/mL) at 37 °C for 48 h at 80–90% confluency.

Each well then received 10 µL of MTT solution (5 mg/mL phosphate buffer saline), and the plate was incubated for two hours in the dark. Subsequently, 100 µL dimethyl sulfoxide (DMSO) was added to solubilize the MTT. The absorbance of each well was measured at 570 nm using a microplate spectrophotometer (BioTek Laboratories, LL, Shoreline, WA, USA). Untreated cells served as the negative control, with all cells in the negative control group remaining viable. The IC_{50} values, representing the concentration of the extract that killed 50% of the cells, were calculated, and the percentage of mitochondrial activities in treated cells was compared to that in untreated cells[60]. The cytotoxic effects of the synthesized AgNPs were also studied following the previous research[61].

The changes in the expression of apoptosis genes (*caspase-3*, *-8 -9*, and *Bax*) and anti-apoptotic genes (*Bcl-xL* and *Bcl-2*) were analyzed using RT-PCR. Cells were cultured in DMEM with 10% FBS. Each extract was administered to the cells in 50 µL amounts based on its IC_{50} value and incubated at 37 °C for 48 h. The morphological changes were observed by the Inverted microscope (Eclipse TS100, Nikon, Japan). The wells were treated with 0.25% trypsin and centrifuged at 12,000 rpm for 8 min. Total RNA was extracted from the resultant pellet using the RNeasy kit (Qiagen, Germany) according to the manufacturer's instructions and subjected to RT-PCR as reported in our previous research[62].

Screening for antibacterial activity

Disc diffusion method

The antibacterial efficacy of the aqueous extract of *A. fragrantissima* and synthesized AgNPs against Gram-positive and Gram-negative pathogens was assessed using the disc-diffusion susceptibility technique, following previously reported protocols[63] with slight modifications. The bacteria tested included Gram-positive strains *S. aureus* (ATCC-29213); *Staphylococcus epidermidis* (MTCC 12228), and *Enterococcus faecalis* (ATCC-29212), and Gram-negative strains *E. coli* (ATCC-25922), *Klebsiella pneumoniae* (MTCC-13883), and *Pseudomonas aeruginosa* (MTCC-27853). The bacterial cultures (0.1 mL, 1×10^6 CFU/mL) were swabbed onto Mueller Hinton Agar (MHA) medium and incubated at 37 °C for 24 h. Sterile paper discs were impregnated with 30 μL of the aqueous extract of *A. fragrantissima* and synthesized AgNPs at concentrations of 500, 1000, and 1500 μg/mL, and incubated for 24 h at 37 °C. For the positive control, 25 μg/mL of ciprofloxacin was used. The extract's ability to inhibit bacteria has been evaluated by measuring the width of the clear zone of inhibition around it in millimeters (mm)[64]. Results were expressed as follows: an inhibition zone diameter ≤ 10 mm for low sensitivity (LS), 10–14 mm for moderate sensitivity (MS), 14–19 mm for sensitivity (S), and ≥ 19 mm for high sensitivity (HS)[65].

Analysis of MIC and MBC

The conventional broth microdilution technique, as published by Basri and Sandra (2016)[66], was used to evaluate the antibacterial characteristics of the aqueous extract of *A. fragrantissima* and the produced AgNPs, with minor adjustments made utilizing the 2,3,5-triphenyl tetrazolium chloride (TTC). TTC staining is a method that uses color changes to distinguish between various cell types' mitochondrial activity. It is a tetrazolium salt that is often used in MIC determination. More specifically, under decreasing circumstances, colorless TTC becomes red. This test quantifies the activity of the cellular mitochondria, more precisely the part played by electron transport system enzymes in the reduction of TTC. The production of a red color signifies the vitality of cells. The indicator's ability to differentiate between metabolically active cells and those that have no metabolism is based on the enzymatic conversion of colorless 2,3,5-triphenyl tetrazolium to reddish-colored 1,3,5-triphenyl formazan in live cells[67,68]. Briefly, Various concentrations of the compounds (1.95 to 800 μg/mL) were prepared in Mueller Hinton broth and dispensed into a 96-well plate well was inoculated with 5×106 CFU/mL bacterial suspension. Ciprofloxacin at a concentration of 25 μg/mL was a positive control, while 0.1% DMSO with Mueller Hinton broth served as a negative control. After 24 h of incubation at 37 °C, the plates were visually assessed for signs of bacterial growth. Following treatment, each well received a working solution containing 2 mg/ml of TTC in PBS and was then incubated at 37 °C for 20 min. Colorless solutions indicate no growth, while pink wells, similar to the positive control indicate bacterial growth. Following a visual assessment of the bacterial growth, the MIC in triplicates was shown to be the minimal concentration that inhibited growth, while the MBC was identified as the lowest concentration at which no growth was observed on an agar subculture[69].

Statistical analysis

Statistical analysis was performed using ANOVA, with results presented as mean $\pm$ SD. A *P* value < 0.05 was considered statistically significant.

Data availability

All data generated or analysed during this study are included in this published article.

References

1. Selwal, N. et al. Enhancing secondary metabolite production in plants: exploring traditional and modern strategies. *J. Agric. Food Res.* **14**, 100702 (2023).
2. Marchev, A. S., Yordanova, Z. P. & Georgiev, M. I. Green (cell) factories for advanced production of plant secondary metabolites. *Crit. Rev. Biotechnol.* **40**, 443–458 (2020).
3. Osman, A. K. E. & Abdein, M. A. E. H. Floristic diversity of Wadi Ar'ar, Saudi Arabia. *J. Taibah Univ. Sci.* **13**, 772–789 (2019).
4. Sayed, O. H. & Masrahi, Y. S. Climatology and phytogeography of Saudi Arabia. A review. *Arid Land. Res. Manag.* **37**, 311–368 (2023).
5. Aati, H., El-Gamal, A., Shaheen, H. & Kayser, O. Traditional use of ethnomedicinal native plants in the Kingdom of Saudi Arabia. *J. Ethnobiol. Ethnomed.* **15**, 1–9 (2019).
6. Barda, C., Grafakou, M. -E., Tomou, E. -M. & Skaltsa, H. Phytochemistry and evidence-based traditional uses of the genus Achillea L.: An update (2011–2021). *Sci. Pharm.* **89**, 50 (2021).
7. Elsharkawy, E. R., Alghanem, S. M. & Elmorsy, E. Effect of habitat variations on the chemical composition, antioxidant, and antimicrobial activities of Achillea fragrantissima (Forssk) Sch. Bip. *Biotechnol. Rep.* **29**, e00581 (2021).
8. Demirci, F., Demirci, B., Gürbüz, İ., Yeşilada, E. & BAŞER K. Characterization and biological activity of Achillea Teretifolia Willd. And A. Nobilis L. subsp. Neilreichii (Kerner) Formanek essential oils. *Turk. J. Biol.*. **33**, 129–136 (2009).
9. Ali, E. M. & Abd El-Moaty, H. Antifungal activity of Achillea Santolina L. and Calendula officinalis L. essential oils and their constituents against fungal infection of liver as complication of cyclophosphamide therapy. *J. Essent. Oil Bear. Plants*. **20**, 1030–1043 (2017).
10. Ozdemir, F. A. Potential effects of essential oil compositions on antibacterial activities of Achillea nobilis L. subsp. Neilreichii. *J. Essent. Oil Bear. Plants*. **22**, 574–580 (2019).
11. Patocka, J. & Navratilova, Z. Achillea fragrantissima: Pharmacology review. *Clin. Oncol.* **4**, 1601 (2019).
12. Benali, T. et al. GC–MS analysis, antioxidant and antimicrobial activities of Achillea odorata subsp. pectinata and Ruta montana essential oils and their potential use as food preservatives. *Foods*. **9**, 668 (2020).
13. Alsohaili, S. Seasonal variation in the chemical composition and antimicrobial activity of essential oil extracted from Achillea fragrantissima grown in northern-eastern Jordanian desert. *J. Essent. Oil Bear. Plants*. **21**, 139–145 (2018).

14. Hijazi, M. A., Jambi, H. A., Aljehany, B. M. & Althaiban, M. A. Potential protective effect of Achillea fragrantissima against adriamycin-induced cardiotoxicity in rats via an antioxidant and anti-inflammatory pathway. *BioMed Res. Int.* **2019**, 5269074 (2019).

15. Sadeq, O. et al. Phytochemical screening, antioxidant and antibacterial activities of pollen extracts from micromeria fruticosa, achillea fragrantissima, and phoenix dactylifera. *Plants.* **10**, 676 (2021).

16. Alasmari, A. Achillea fragrantissima (Forssk.) Sch. Bip instigates the ROS/FADD/c-PARP expression that triggers apoptosis in breast cancer cell (MCF-7). *Plos One.* **19**, e0304072 (2024).

17. Al-Gaby, A. M. & Allam, R. R. Chemical analysis, antimicrobial activity, and the essential oils from some wild herbs in Egypt. *J. Herbs Spices Med. Plants.* **7**, 15–23 (2000).

18. Zeedan, G., Abdalhamed, A., Ottai, M., Abdelshafy, S. & Abdeen, E. Antimicrobial, antiviral activity and GC-MS analysis of essential oil extracted from Achillea fragrantissima plant growing in Sinai Peninsula. *Egypt. J. Microb. Biochem. Technol. S* **8**, (2014).

19. Yien, R. M. K. et al. Nanotechnology promoting the development of products from the biodiversity of the Asteraceae family. *Nutrients.* **15**, 1610 (2023).

20. Baharara, J., Namvar, F., Ramezani, T., Mousavi, M. & Mohamad, R. Silver nanoparticles biosynthesized using Achillea biebersteinii flower extract: apoptosis induction in MCF-7 cells via caspase activation and regulation of Bax and Bcl-2 gene expression. *Molecules.* **20**, 2693–2706 (2015).

21. Chahrdoli, A. et al. Achillea Wilhelmsii C. Koch mediated blood compatible silver nanoparticles. *Mater. Today Commun.* **25**, 101577 (2020).

22. Karimi, S. & Mahdavi Shahri, M. Medical and cytotoxicity effects of green synthesized silver nanoparticles using Achillea millefolium extract on MOLT-4 lymphoblastic leukemia cell line. *J. Med. Virol.* **93**, 3899–3906 (2021).

23. Bayda, S., Adeel, M., Tuccinardi, T., Cordani, M. & Rizzolio, F. The history of nanoscience and nanotechnology: From chemical–physical applications to nanomedicine. *Molecules.* **25**, 112 (2019).

24. Gupta, D., Thakur, A. & Gupta, T. K. Green and sustainable synthesis of nanomaterials: Recent advancements and limitations. *Environ. Res.* **116316** (2023).

25. Kumar, K. M. et al. Green synthesis of silver nanoparticles using Terminalia chebula extract at room temperature and their antimicrobial studies. *Spectrochim. Acta Part A Mol. Biomol. Spectrosc.* **91**, 228–233 (2012).

26. Mani, M. et al. Studies on the spectrometric analysis of metallic silver nanoparticles (Ag NPs) using Basella alba leaf for the antibacterial activities. *Environ. Res.* **199**, 111274 (2021).

27. Azizi, S., Namvar, F., Mahdavi, M., Ahmad, M. B. & Mohamad, R. Biosynthesis of silver nanoparticles using brown marine macroalga, Sargassum muticum aqueous extract. *Materials.* **6**, 5942–5950 (2013).

28. Nasrollahzadeh, M., Sajadi, S. M. & Maham, M. Tamarix gallica leaf extract mediated novel route for green synthesis of CuO nanoparticles and their application for N-arylation of nitrogen-containing heterocycles under ligand-free conditions. *RSC Adv.* **5**, 40628–40635 (2015).

29. Momeni, S. S., Nasrollahzadeh, M. & Rustaiyan, A. Green synthesis of the Cu/ZnO nanoparticles mediated by Euphorbia prolifera leaf extract and investigation of their catalytic activity. *J. Colloid Interface Sci.* **472**, 173–179 (2016).

30. Rehan, M., Mashaly, H. M., Abdel-Aziz, M. S., Abdelhameed, R. M. & Montaser, A. S. Viscose fibers decorated with silver nanoparticles via an in-situ green route: UV protection, antioxidant activities, antimicrobial properties, and sensing response. *Cellulose.* 1–32 (2024).

31. Baharara, J., Namvar, F., Ramezani, T., Hosseini, N. & Mohamad, R. Green synthesis of silver nanoparticles using Achillea biebersteinii flower extract and its anti-angiogenic properties in the rat aortic ring model. *Molecules.* **19**, 4624–4634 (2014).

32. Pechyen, C. et al. Green biosynthesis of silver nanoparticles from aqueous Zingiber montanum flower extract for enhanced application in medical diagnostic biosensors. *J. Mater. Sci. Mater. Electron.* **35**, 507 (2024).

33. Eid, A. M. et al. Endophytic Streptomyces laurentii mediated green synthesis of Ag-NPs with antibacterial and anticancer properties for developing functional textile fabric properties. *Antibiotics.* **9**, 641 (2020).

34. Yin, I. X. et al. The antibacterial mechanism of silver nanoparticles and its application in dentistry. *Int. J. Nanomed.* 2555–2562 (2020).

35. Additives EPo, et al. Safety and efficacy of feed additives consisting of essential oils derived from the flower buds or the leaves of Syzygium aromaticum (L.) Merr. & LM Perry (clove bud oil and clove leaf oils) for all animal species (FEFANA asbl). *EFSA J.* **21**, e08183 (2023).

36. Hirasawa, K. et al. Macrolide antibiotics exhibit cytotoxic effect under amino acid-depleted culture condition by blocking autophagy flux in head and neck squamous cell carcinoma cell lines. *PLoS One.* **11**, e0164529 (2016).

37. Awad, B. M. et al. Cytotoxic activity evaluation and molecular docking study of phenolic derivatives from Achillea fragrantissima (Forssk.) Growing in Egypt. *Med. Chem. Res.* **26**, 2065–2073 (2017).

38. Abd-ElGawad, A. M. et al. Achillea fragrantissima essential oil, wild grown in Saudi Arabia and Egypt: Detailed comparative chemical profiling, and evaluation of Allelopathic, antioxidant, and Antibacterial activities. *Chemistry.* **5**, 2347–2361 (2023).

39. Ullah, A. et al. Important flavonoids and their role as a therapeutic agent. *Molecules.* **25**, 5243 (2020).

40. Akbari, B., Baghaei-Yazdi, N., Bahmaie, M. & Mahdavi Abhari, F. The role of plant-derived natural antioxidants in reduction of oxidative stress. *BioFactors.* **48**, 611–633 (2022).

41. Alenad, A. M. et al. Achillea fragrantissima extract exerts its anticancer effect via induction of differentiation, cell cycle arrest and apoptosis in chronic myeloid leukemia (CML) cell line K562. *J. Med. Plants Res.* **7**, 1561–1567 (2013).

42. Break, M. K. B. et al. Achillea fragrantissima (Forssk.) Sch. Bip. Methanolic extract exerts potent antimicrobial activity and causes cancer cell death via induction of caspase-dependent apoptosis and S-phase arrest. *Nat. Prod. Res.* **36**, 4639–4644 (2021).

43. Alshuail, N. et al. Achillea fragrantissima (Forssk.) Sch. Bip flower dichloromethane extract exerts anti-proliferative and pro-apoptotic properties in human triple-negative breast cancer (MDA-MB-231) cells: In Vitro and in Silico studies. *Pharmaceuticals.* **15**, 1060 (2022).

44. Sharifi-Rad, M., Elshafie, H. S. & Pohl, P. Green synthesis of silver nanoparticles (AgNPs) by Lallemantia royleana leaf extract: their bio-pharmaceutical and catalytic properties. *J. Photochem. Photobiol. A Chem.* **448**, 115318 (2024).

45. Shashiraj, K. N. et al. Rotheca Serrata flower bud extract mediated bio-friendly preparation of silver nanoparticles: Their characterizations, anticancer, and apoptosis inducing ability against pancreatic ductal adenocarcinoma cell line. *Processes.* **11**, 893 (2023).

46. Amini Navaie, B. et al. Antioxidant and cytotoxic effect of aqueous and hydroalcoholic extracts of the Achillea millefolium L. on MCF-7 breast cancer cell line. *Int. Biol. Biomed. J.* **1**, 119–125 (2015).

47. Math, H. H. et al. Investigation of in vitro anticancer and apoptotic potential of biofabricated silver nanoparticles from Cardamine hirsuta (L.) leaf extract against Caco-2 cell line. *Inorganics.* **11**, 322 (2023).

48. Bhat, M. et al. Biogenic synthesis, characterization and antimicrobial activity of Ixora brachypoda (DC) leaf extract mediated silver nanoparticles. *J. King Saud Univ. Sci.*. **33**, 101296 (2021).

49. Sharifi-Rad, M., Pohl, P., Epifano, F. & Álvarez-Suarez, J. M. Green synthesis of silver nanoparticles using Astragalus tribuloides delile. Root extract: Characterization, antioxidant, antibacterial, and anti-inflammatory activities. *Nanomaterials.* **10**, 2383 (2020).

50. Sharifi-Rad, M., Pohl, P. & Epifano, F. Phytofabrication of silver nanoparticles (AgNPs) with pharmaceutical capabilities using Otostegia persica (Burm.) Boiss. Leaf extract. *Nanomaterials.* **11**, 1045 (2021).

51. Sharifi-Rad, M. & Pohl, P. Synthesis of biogenic silver nanoparticles (Agcl-NPs) using a pulicaria vulgaris gaertn. Aerial part extract and their application as antibacterial, antifungal and antioxidant agents. *Nanomaterials.* **10**, 638 (2020).

52. Essghaier, B., Hannachi, H., Nouir, R., Mottola, F. & Rocco, L. Green Synthesis and characterization of Novel Silver nanoparticles using Achillea maritima subsp. maritima Aqueous Extract: antioxidant and antidiabetic potential and effect on virulence mechanisms of bacterial and fungal pathogens. *Nanomaterials.* **13**, 1964 (2023).

53. Roy, A., Bulut, O., Some, S., Mandal, A. K. & Yilmaz, M. D. Green synthesis of silver nanoparticles: biomolecule-nanoparticle organizations targeting antimicrobial activity. *RSC Adv.* **9**, 2673–2702 (2019).

54. Quevedo, A. C. et al. UV-Vis spectroscopic characterization of nanomaterials in aqueous media. *JoVE (J. Vis. Exp.)* e61764 (2021).

55. Al-Otibi, F. O., Alrumaizan, G. I. & Alharbi, R. I. Evaluation of anticandidal activities and phytochemical examination of extracts prepared from Vitex agnus-castus: a possible alternative in treating candidiasis infections. *BMC Complement. Med. Ther.* **22**, 69 (2022).

56. Wolfe, K. L. & Liu, R. H. Apple peels as a value-added food ingredient. *J. Agric. Food Chem.* **51**, 1676–1683 (2003).

57. Chang, C. -C., Yang, M. -H., Wen, H. -M. & Chern, J. -C. .Estimation of total flavonoid content in propolis by two complementary colorimetric methods. *J. Food Drug Anal.* **10**, (2002).

58. Mosmann, T. Rapid colorimetric assay for cellular growth and survival: Application to proliferation and cytotoxicity assays. *J. Immunol. Methods.* **65**, 55–63 (1983).

59. Alkhudhayri, A. A., Wahab, R., Siddiqui, M. A. & Ahmad, J. Selenium nanoparticles induce cytotoxicity and apoptosis in human breast cancer (MCF-7) and liver (HEPG2) cell lines. *Nanosci. Nanatechnol. Lett.* **12**, 324–330 (2020).

60. Al-Dhabi, N. A. & Valan Arasu, M. Quantification of phytochemicals from commercial Spirulina products and their antioxidant activities. *Evid.-Based Complement. Altern. Med.* **2016** (2016).

61. Ahn, S. et al. Rg5: Rk1 attenuates TNF-α/IFN-γ-induced production of thymus-and activation-regulated chemokine (TARC/CCL17) and LPS-induced NO production via downregulation of NF-κB/p38 MAPK/STAT1 signaling in human keratinocytes and macrophages. *Vitro Cell. Dev. Biol.-Anim..* **52**, 287–295 (2016).

62. Aziz, I. M. et al. Chemical composition, antioxidant, Anticancer, and antibacterial activities of roots and seeds of Ammi visnaga L. methanol extract. *Pharmaceuticals.* **17**, 121 (2024).

63. Al-Dhabi, N. A. et al. Probiotic and antioxidant potential of Lactobacillus reuteri LR12 and Lactobacillus lactis LL10 isolated from pineapple puree and quality analysis of pineapple-flavored goat milk yoghurt during storage. *Microorganisms.* **8**, 1461 (2020).

64. Singh, P. et al. Extracellular synthesis of silver and gold nanoparticles by Sporosarcina koreensis DC4 and their biological applications. *Enzym. Microb. Technol.* **86**, 75–83 (2016).

65. Zhou, G. et al. Induction of maggot antimicrobial peptides and treatment effect inSalmonella pullorum-infected chickens. *J. Appl. Poult. Res.* **23**, 376–383 (2014).

66. Basri, D. F. & Sandra, V. Synergistic interaction of methanol extract from Canarium odontophyllum Miq. Leaf in combination with oxacillin against methicillin-resistant Staphylococcus aureus (MRSA) ATCC 33591. *Int. J. Microbiol.* (2016).

67. Gabrielson, J. et al. Evaluation of redox indicators and the use of digital scanners and spectrophotometer for quantification of microbial growth in microplates. *J. Microbiol. Methods.* **50**, 63–73 (2002).

68. Veiga, A. et al. Colorimetric microdilution assay: validation of a standard method for determination of MIC, IC50%, and IC90% of antimicrobial compounds. *J. Microbiol. Methods.* **162**, 50–61 (2019).

69. Aljeldah, M. M., Yassin, M. T., Mostafa, A. A. F. & Aboul-Soud, M. A. Synergistic antibacterial potential of Greenly Synthesized Silver nanoparticles with Fosfomycin against some nosocomial bacterial pathogens. *Infect. Drug Resist.* 125–142 (2022).

Acknowledgements

Author contributions

M.F.A, H.A.A and I.M.A. wrote the main manuscript text. I.M.A, M.F.A, F.A., and N.A.A. Mainly responsible for providing data. R.M.A., S.M.A., and H.R. are responsible for charting. All authors reviewed the manuscript.

Funding

Declarations

Competing interests

The authors declare no competing interests.

Ethical approval

Not applicable.

Additional information

Correspondence and requests for materials should be addressed to I.M.A.

Reprints and permissions information is available at www.nature.com/reprints.

Publisher's note Springer Nature remains neutral with regard to jurisdictional claims in published maps and institutional affiliations.